UNIVERSIDAD DE CANTABRIA

Departamento de Ciencias y Técnicas del Agua y del Medio Ambiente

Numerical modeling of the global wave climate variability and associated environmental and technological risks

---

A Doctoral Thesis by: Borja González Reguero

Advisors: Iñigo J. Losada and Fernando J. Méndez

Santander, December, 2012

Chapter 3

Wave climatology

"A perfection of means, and confusion of aims, seems to be our main problem"

Albert Einstein

3.1 Introduction

Understanding of mean and extreme conditions of waves is of interest not only for the scientific community but also for engineering and maritime purposes. The range of applications requiring reliable information on ocean wave climate is wide.

Changing wind systems projected to occur with climate change will have the effect of altering the surface ocean wave energy felt on global coasts. These changes must be quantified in order to assess the ocean wave resources available for renewable wave energy generation, and to enable coastal managers and researchers to determine how changes in global wave climate will impact on coastal infrastructure and the environment.

Several global wave climatology descriptive studies have been published in recent years, see for instance: [Barstow, 1996, Young, 1999, Sterl and Caires, 2005, Semedo et al., 2011b, Young et al., 2011]. Global studies are generally based on two types of data: satellite altimeter observations and numerical modeling reanalysis. Other works have been based on buoy measurements or ship observations data ([Gulev and Grigorieva, 2004, Gulev and Grigorieva, 2006]), but they incur in scarceness and non-homogeneous spatial distribution of the data. The development of long-term reanalysis datasets over the last two decades have changed the investigation approaches of climate variability and long-term analysis. Nowadays, it can be stated that wave reanalysis complemented with altimeter and buoy measurements are the best information for global studies of wave climate.

One aspect of wave climatology, often understudied but with challenging interest, is wave direction. The variability of wave direction is probably the most important aspect defining the influence of a changing climate on coastal zones. The essential drawback is that directional data

are particularly sparse globally and not registered by altimeter measurements. This fact makes the global reanalysis the best source of wave directional information so far.

Another important aspect in the study of global wave climate is the variations occurring in a scale longer than a year, usually known as *inter-annual variability*. Since waves are primarily derived from cyclonic and anti-cyclonic conditions in the global oceans, links are expected between mean sea level conditions inter-annual anomalies (pressure and temperature) and wave climate. Understanding those links between wave climate and climatic oscillations has been usually constrained by the length and resolution of wave measurements (usually buoys). Wave reanalysis of global wave climate also address those limitations. [Hemer et al., 2007] and [Hemer et al., 2008] study wave climate variability in the Southern Hemisphere (SH) using the C-ERA-40 ([Uppala et al., 2005]) reanalysis data. Ocean wave heights have been often correlated with inter-annual climate variations such as the North Atlantic Oscillation ([Woolf and Challenor, 2002, Dodet et al., 2010]) or the Southern Annular Mode ([Hemer et al., 2010]). More recently, [Semedo et al., 2011b] extended the study of teleconnections based on the former reanalysis to global ocean. [Izaguirre et al., 2011] explain widely the variability in extreme wave heights for several climate indices globally by using altimeter information. Other prior studies on extreme wave climate and teleconnections are [Wang and Swail, 2001] and [Menendez et al., 2008].

In the present chapter we extend the study of teleconnections of many of the most important climate patterns and several wave height statistics and, for the first time, to the global wave energy direction. Many important patterns are identified for the Northern and Southern Hemispheres as well as other regional features in several ocean basins, with outstanding consequences in the coastal zones.

Ocean wave height changes are important to be evaluated for understanding impacts of possible changes. Long-term changes of storm waves are important for infrastructures in the coastal zones (e.g. ports, wave energy farms, coastal development, etc.). Coastal erosion is another issue of concern for the years to come, with currently more than 70% of sandy beaches subjected to erosion ([Bird, 1985]). Previous investigations on trends in oceanic wave heights used ship observations [Gulev and Grigorieva, 2004, Gulev and Grigorieva, 2006], buoy measurements, numerical modeling [Group, 1998, Cox and Swail, 2001, Wang and Swail, 2001, Wang and Swail, 2002, Sterl and Caires, 2005, Hemer et al., 2010, Dodet et al., 2010, Semedo et al., 2011b] or satellite altimeter observations [Young et al., 2011]. Independently of the source of information, the numerous studies show an increasing trend in significant wave height especially in the North-Atlantic and North-Pacific. However, most studies are regional rather than global. The study of long-term trends on a global scale is based on the GOW wave reanalysis for a total of 61 years (1948-2008).

The aim of the present chapter is to describe global wave climatology for the last six decades to study the natural inter-annual variability of wave heights and wave directions, as to identify the long-term trends in several wave statistics, extreme events and wave climate storminess. The work is structured in several sections. The section that follows this introduction explains the data employed in the analysis. Section 3.3 addresses the description of wave climatology through several wave heights statistics, mean energy flux direction and corresponding standard deviations. Wave climate inter-annual variability is studied in section 3.4 by identifying correlation patterns

of wave heights and mean energy flux direction with several of the most important climate patterns affecting the global ocean. Section 3.5 presents results for the long-term changes in wave heights, wave directions and extreme events. Owing to the great influence of climate patterns in wave climatology, and to complete the picture, a brief review is provided on anthropogenically-forced changes in climate variability in section 3.6. A discussion on wave energy, its natural past variability and possible influence of climate change is held on section 3.7. Finally, main conclusions are offered in Section 3.8.

3.2 Data sources

3.2.1 Altimeter derived significant wave heights

In contrast with buoy data, altimetry wave measurements provide the best possible spatial coverage for global studies. From the nineties, different satellite missions (Jason 1, Jason 2, TOPEX, ERS-2, Envisat and GFO) incorporate altimetry sensors. Provided the corrections in the literature are applied, the wave height data show very good agreement between missions and, consequently, they are combined for comparison with the reanalysis results.

A severe limitation of satellite altimetry data is the sparseness of the measurements both in time and space. [Woolf and Challenor, 2002] indicated the necessity of a calibration of the altimeter wave heights for an adequate wave climate description. For this reason, wave altimeter data have been corrected using the calibration procedures summarized in [Cotton, 1998] and [Woolf and Challenor, 2002], and later updated by [Hemer et al., 2010] with extra years and additional satellite missions.

In this study, we have used the mentioned six satellite missions covering the period from 1992 to 2008 to perform a spatial correction of the reanalysis wave heights as explained in chapter 2.

3.2.2 Buoy data

The study of variability and trends of directional wave climate relies on the quality of the analysis data. Buoy data are the available measurements with the highest degree of confidence but, unfortunately, very few deep water buoys exist with sufficient time history for long-term trend analysis. When considering directional wave climate, the number of measurements is even more scarce. For a global scale analysis, buoy data are not suitable and other sources of data must be used. Nevertheless, buoy data constitute a valuable data for comparison with other dataset owing to its high quality degree (see chapter 2). In-situ buoy measured wave data used in this work have been obtained from three different sources: NOAA National Data Buoy Center, the Environment Canada and OPPE (Spain).

3.2.3 Wave reanalysis data

Numerical reanalysis constitutes a valuable source of information for climatology characterization and long-term changes and trends ([Weisse and Von Storch, 2010]). In this work, the temporal variability and change of global wave climate are explored using wave data from a 61-year wave reanalysis (GOW, Global Ocean Waves reanalysis, developed in Chapter 2). As has been shown, the GOW database ([Reguero et al., 2012b]) is obtained with the WaveWatch III model ([Tolman, 2002a, Tolman, 2002b, Tolman et al., 2002]; denoted as WW3 in the following) and using the NCEP/NCAR ([Kalnay et al., 1996]) global winds and ice cover datasets. Simulations are computed on a global grid with a spatial resolution of 1.5° in longitude and 1° in latitude. GOW reanalysis provides hourly wave climate parameters (significant wave height, H_s; mean period; peak frequency; mean direction and peak direction) from 1948 onwards. Wave heights are calibrated with altimeter observations through a correction depending on wave direction [Mínguez et al., 2011] and where outliers due to tropical cyclones (not simulated) are identified and discarded using the method proposed by [Mínguez et al., 2012], as explained in Chapter 2.

Validation using measurements from buoys and altimeters indicates that both wave heights and wave directions are reasonably well represented across the different time-scales involved: from hours to months, seasons and years (see chapter 2 or [Reguero et al., 2012b]). Although special attention must be taken when analyzing the Southern Hemisphere (SH) due to inhomogeneities in the reanalyzed winds, the dataset is appropriate for the determination of trends and variability, taking into consideration its spatial and temporal coverage and the validations performed.

3.2.4 Climate indices

In this study, different climate indices are used to investigate the inter-annual variability in the global wave climate, hereafter listed: the Atlantic Multidecadal Oscillation (AMO); the Arctic Oscillation (AO); the East Atlantic oscillation (EA); the North Atlantic Oscillation (NAO); the ENSO phenomenon (El Niño Southern Oscillation) measured by the index NIÑO3; the Pacific-North America Index (PNA); the Southern Hemisphere Annular Mode (SAM) or also referred to as the Antarctic Oscillation (AAO); the Scandinavian index (SCA); the Southern Oscillation Index (SOI); the Western Pacific index (WP); the Tropical North Atlantic index (TNA); the East Pacific - North Pacific (EP-NP); the Indian Ocean Dipole (IOD) measured through the Dipole Mode Index (DMI); and the Quasi-Biennial Oscillation (QBO). Only the most extended and prominent patterns of influence are shown in the results. When not shown, it indicates that only regional features or no statistically significant relationship were found.

For a comprehensive list and explanation of these and other climate indices, the NOAA-National Weather Service (www.cpc.ncep.noaa.gov) can be consulted for further details.

Climate indices time series were obtained from several sources. SAM was selected from the British Antarctic Survey (www.nerc-bas-ac-uk/icd/gjma); DMI from the Japan Marine Science and Technology Center (www.jamstec.go.jp); the NAO from the Climate Research Unit of the University of East Anglia (www.cru.uea.ac.uk/cru); and the rest of the indices from the NOAA-National Weather Service (www.cpc.ncep.noaa.gov).

3.3 Global Wave Climatology

3.3.1 Mean global wave heights and seasonal variations

Many studies have described wave climatology during the last years, some of them at a global scale [Barstow, 1996, Young, 1999, Cox and Swail, 2001, Caires et al., 2004b, Semedo et al., 2011b] and others focusing on extreme wave height values [Alves and Young, 2004, Chen et al., 2004, Sterl and Caires, 2005, Caires and Sterl, 2005a, Izaguirre et al., 2011]. This work addresses the description of the global wind-waves climatology considering several statistics and their standard deviations computed over the last six decades with a clear objective: to describe the mean global conditions and the variability of waves on a global perspective, covering monthly, seasonal and inter-annual time scales.

Corrected data from the numerical wave reanalysis (i.e. incorporating altimeter based corrections) are temporally averaged (i.e. monthly, seasonally and annually) and the inter-annual standard deviations are determined as the mean standard deviations of each time block. Figures 3.1 and 3.2 display the mean annual significant wave height (H_s) and its 90^{th} percentile, respectively, along with their corresponding standard deviations globally.

The seasonal global maps of H_s are displayed in Figure 3.3, representing the mean value for each season, which are defined as December, January and February (DJF); March, April and May (MAM); June, July and August (JJA) and September, October and November (SON).

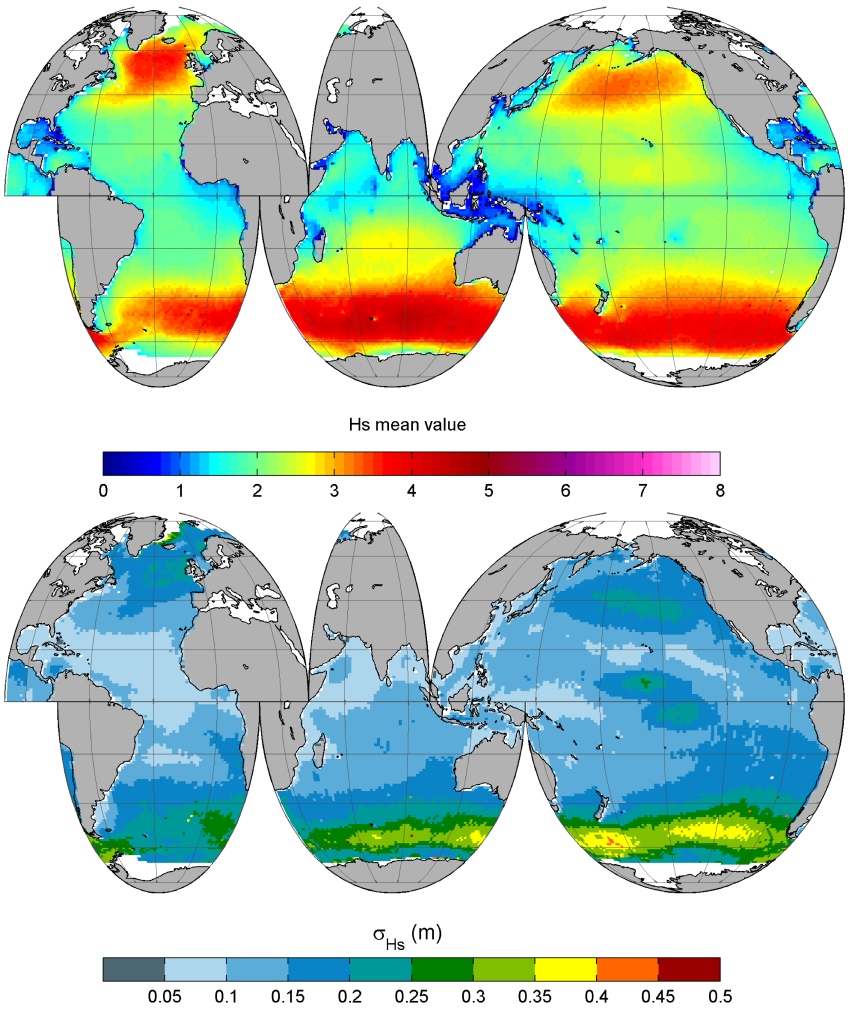

Figure 3.1: Annual mean significant wave height (upper panel) and standard deviation (lower panel) in m.

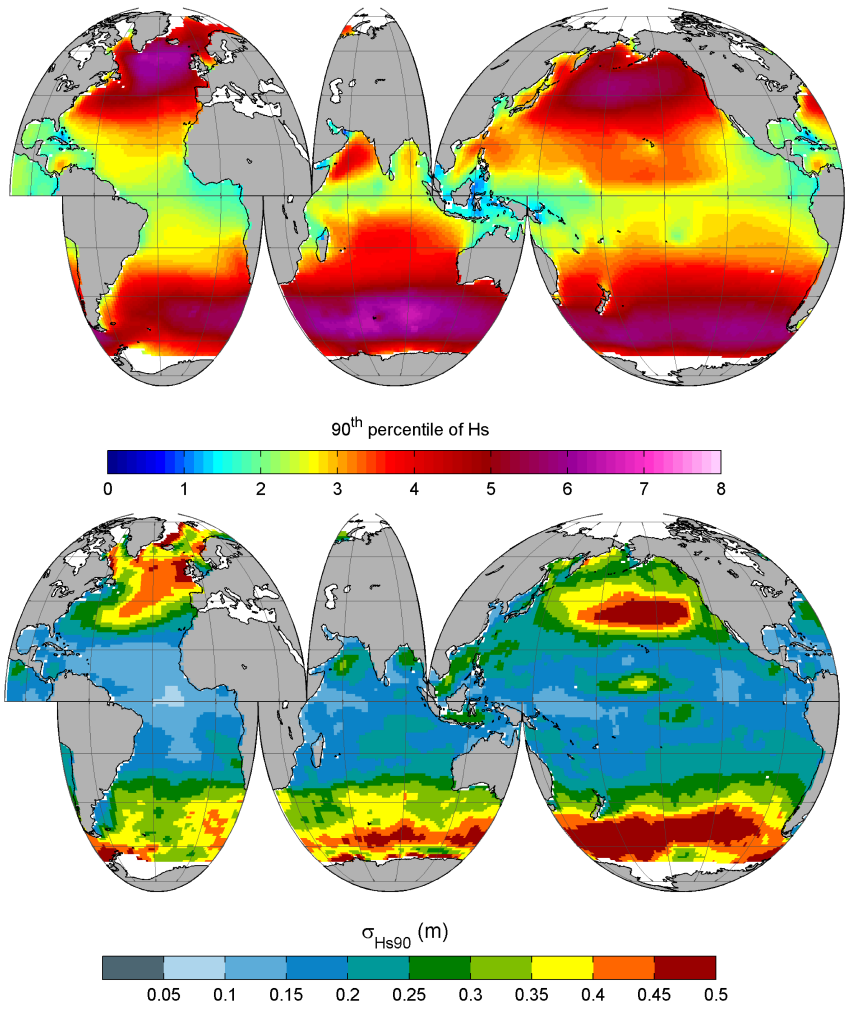

Figure 3.2: Annual 95^{th} percentile of significant wave height (upper panel) and standard deviation (lower panel) in m.

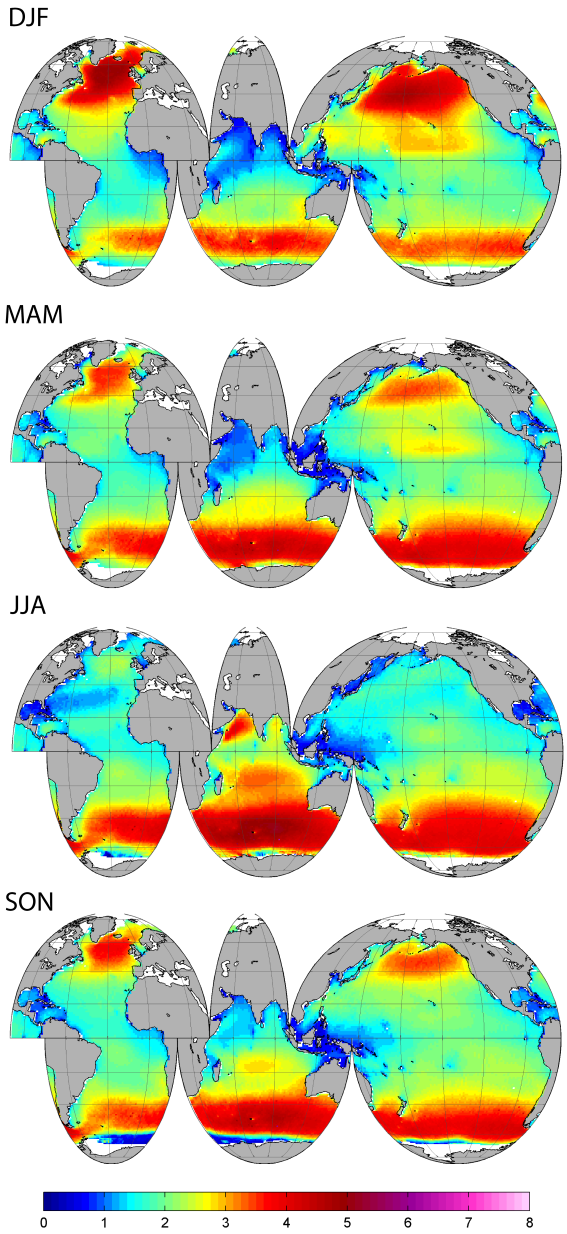

Figure 3.3: Seasonal mean significant wave height (in m).

The general pattern in these maps representing wave height parameters are dominated by large zonal features with a clear poleward increase. Maximum values are found during each respective hemisphere winter, located in the North Pacific around the 50°N, in the North Atlantic at about 60°N and in the SH between 40 and 60°S. The extension and intensity of these areas vary within seasons as can be clearly seen in Figure 3.3. The storms in the North Pacific and North Atlantic generate waves during winter ([Young, 1999, Semedo et al., 2011b]) with a mean seasonal value of around 5 m, while during the summer the wave climate is considerable smoother because: (1) the storm track activity is much weaker and (2) it shifts poleward ([Trenberth, 1991, Semedo et al., 2011b]). In the Southern Hemisphere (SH) the seasonal average values of the wave height remain about 5 m but the extension of the area with these strong conditions gets wider latitudinally, extending northwards in more than 10° during the austral winter. The reason for this lies on the storm-track activity which is remarkably persistent throughout the year in the SH, both in location and intensity. [Trenberth, 1991] found that storm track activity extends over a broader range of latitudes during winter mainly due to the polar jet stream. The storm track remains near 50°S year round, being more intense in the southern Indian Ocean while weakening in the South Pacific. This process conducts to generation of waves eastwards during all seasons. Consequently, minimum values of wave heights are found in the equatorial areas of the eastern Pacific, eastern Atlantic, northern Indian Ocean and Java and Flores seas.

Striking regional features are identified in the Polynesian Archipelago and the Caribbean Sea with mean annual values below 1 m and reaching around 2 m of H_s during MAM and JJA in the South Caribbean and south Java Sea. Another regional feature that is worth noting is the 4 m wave height average values occurring in the Arabian sea during JJA, mainly associated with the Indian monsoon, as a local effect of wind generation in that particular area. It has to be noticed that lower heights, around 3 m of H_s, are found in the C-ERA-40 dataset for this particular region [Semedo et al., 2011b]. Although this difference may be due to wind forcing fields, it is a relevant discrepancy indeed. The spatial pattern for both datasets keep great similarities though.

As a conclusion, it can be said that the Northern Hemisphere (NH) presents a considerable higher range of variability between smooth and rough conditions of wave heights than the SH, as previously seen in other works ([Semedo et al., 2011b, Chen et al., 2004, Caires and Sterl, 2005a]). This is clearly reflected in the standard deviation of annual mean and the 90^{th} percentile of H_s, where the maximum deviations are displaced from the center of maximum mean values, while in the SH both areas coincide in location. The North Indian Ocean is another area of the Globe with a considerable wide range of seasonal variation in wave heights and between mean and high tail distribution values.

Regarding the major differences in the NH between the 90^{th} percentile and the annual mean of H_s, as previously noted by [Chen et al., 2004, Alves and Young, 2004] and [Caires and Sterl, 2005a], NH presents maximum return values of wind and waves in spite of not presenting either the highest wind climatology nor the greatest wind variability among the world's oceans. This fact also seems to indicate an important contribution of inter-annual variability for the extreme values.

3.3.2 Wave period

Wave climate can not be only characterized by wave heights statistics. Wave periods are another parameter worth analyzing as it is critical for wave energy transformation and swell characterization, as usually evidenced on surf conditions along the world coastline. From their generation waves propagate throughout the global oceans being dispersed by their different frequencies, defining the sea and swell sea-states. The areas distant from generation are affected by swells sea-states being characterized by longer wave periods. As this occurs, the wave period plays a role as an indicator of the relative weight of swell at each region of the global ocean. The relation between the peak and the mean periods also provides information about the type of energy spectrum. The mean and peak periods are analyzed below to provide a general view on these relevant issues.

Figure 3.4 represents the mean of the annual mean period and its standard deviation. Eastern areas of the Pacific, Atlantic and Indian oceans present the largest values of mean periods over 11 s. Meanwhile, the western margin of the main ocean basins present periods in the range from 7 to 9 s. Islands shadowing at the main archipelagos of the world provides protection from ocean swell propagation in seas like the Caribbean or the sea of Japan, where periods remain below 6 s. Low dispersion is detected in the annual mean period time series as the standard deviation shows values of about 1 s for the western regions of the oceans, around 1.6 s on the eastern side and only reaching 2 s in particular locations which are: west of Madagascar, the Arabian sea, the Bay of Bengal and the north-west of Australia, in the Indian Ocean; eastern margin of the North-Atlantic; and equatorial Pacific America region.

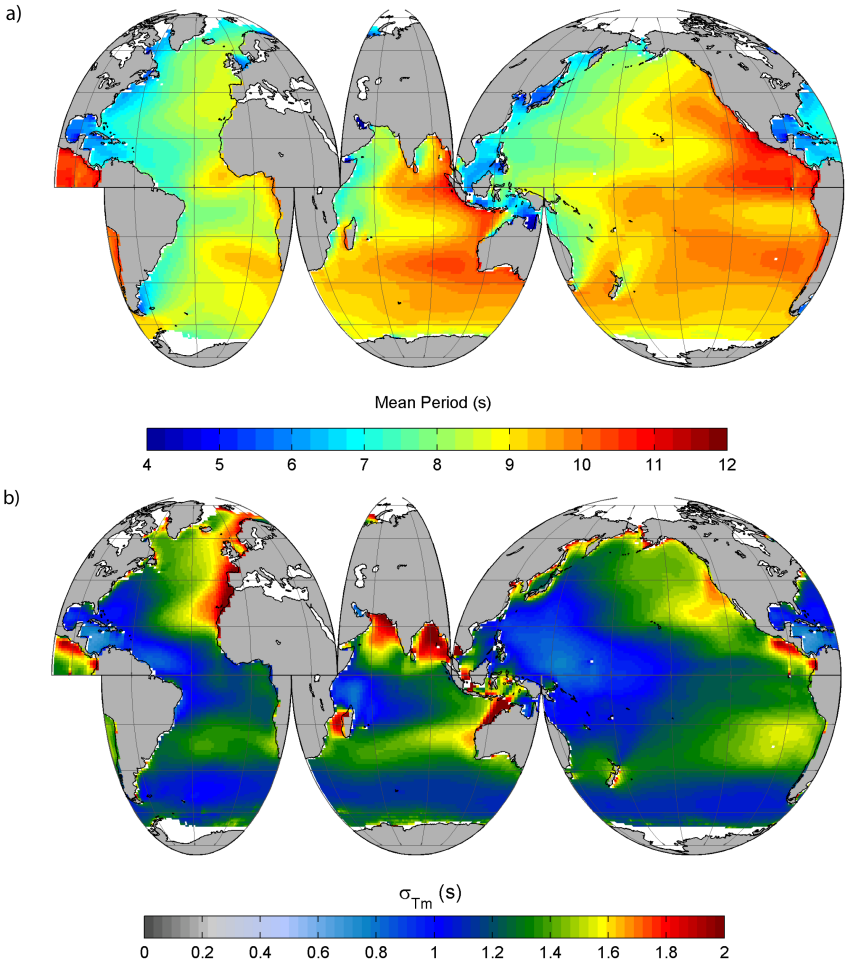

Figure 3.4: Annual mean value of mean period (panel a) and standard deviation (panel b), in seconds.

Peak periods, shown in Figure 3.5, keep patterns with great similarities to the mean period. This time, however, values reach 13 to 14 s in the eastern areas of the oceans. Dispersion is in this case larger and about 2 s generally, reaching 3 s at the eastern regions and 4 s on the bay of Bengal and the north-west of Australia.

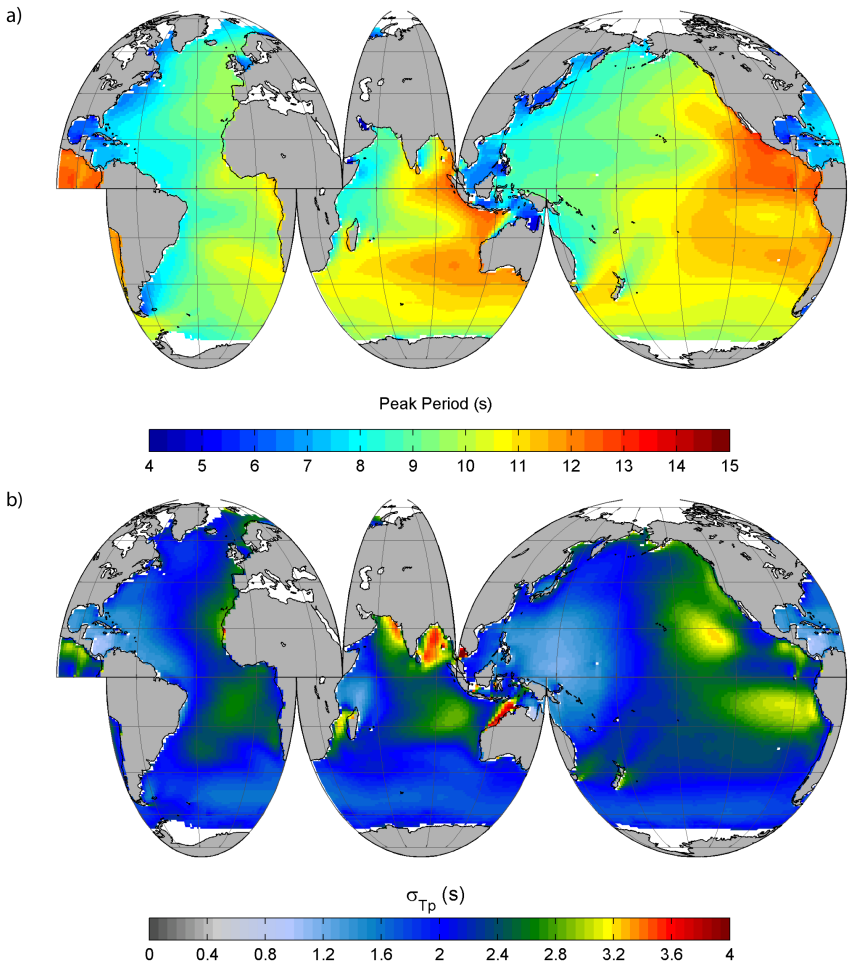

Figure 3.5: Annual mean value of peak period (panel a) and standard deviation (panel b), in seconds.

The ratio between peak and mean periods provides information about the shape of the frequency spectra. This ratio is depicted in Figure 3.6. High latitudes western areas of the oceans are characterized by annual peak periods up to a 10 % higher than the mean periods, clearly indicating lower dispersion of waves. The effect of westerlies on the swell generation (especially from the SH) results in a 20 % higher peak periods in the eastern Pacific, the Timor sea and the Gulf of Guinea. This fact evidences that in these areas the peak of wave energy is concentrated on the higher periods meaning that coastal areas in the region are affected by the longest swell waves in the world. These areas in the Atlantic and the Pacific are commonly known as "swell pools".

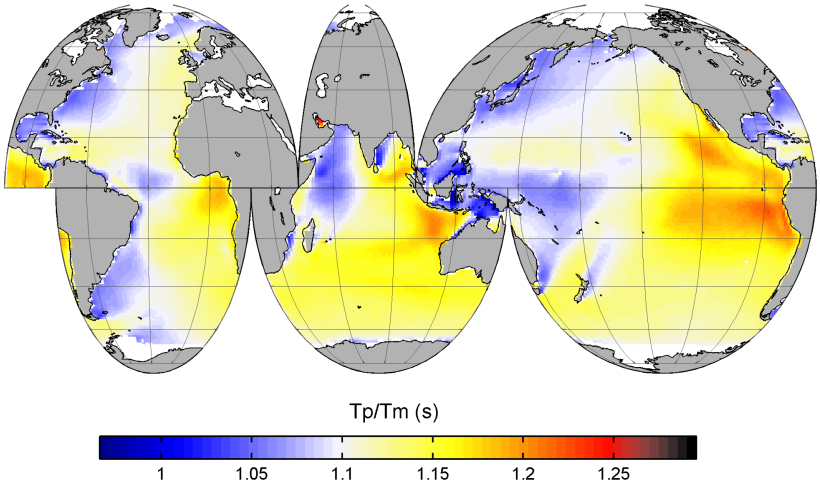

Figure 3.6: Ratio between the annual mean values of peak period over the mean period.

For a complete analysis of wave and wind climatology and swell dominance [Young, 1999, Alves, 2006] and [Semedo et al., 2011b] can be consulted. The results here shown are in agreement with existing literature.

3.3.3 Directional wave climate

3.3.3.1 Global directional wave climate

Concern about directional wave climate has traditionally received less attention than other wave parameters, possibly due to the lack of information in wave direction and appropriate spatial and temporal scales. Although the coastal implications of wave directions variability are of primary importance, specific studies on this subject are scarce. In the present section, we explore this matter on a global perspective and for different temporal scales.

Other previous works usually consider the mean wave direction as the directional descriptor of wave climate. However, in this work it is considered that the mean direction of the energy is more representative of the dominant wave climate. For example, this variable is important for the coastal system because it is intimately related with changes in form of beaches. Therefore, to describe the directional wave climate the mean annual direction of the wave Energy Flux (EF) is analyzed, which is obtained, according to [Holthuijsen, 2007], as:

$$EF = E \cdot c_g = \rho g H_s^2 c_g / 8 \tag{3.1}$$

where E represents the wave energy density, c_g the group wave celerity, g the gravitational acceleration and ρ is the sea water density. The EF can be considered a vector traveling in the direction of waves (α). So, the mean direction of the EF is given by:

$$\theta_{EF} = \arctan \frac{\sum EF(t) \cdot \sin \alpha \cdot \triangle t}{\sum EF(t) \cdot \cos \alpha \cdot \triangle t} \tag{3.2}$$

The annual time series of the mean direction of EF during the period from 1948 to 2008 are obtained for trend analysis and wave climatology description purposes. The monthly distribution of this variable is also computed to study correlation with several climate indices (monthly time series).

Figure 3.7 shows the annual mean and the standard deviation of the energy flux direction, expressed in degrees from North (90° for waves coming from east). Two striking points of change are worth noting in the annual mean energy flux direction. The first one is found near the equatorial African border and coincides with the Atlantic "swell pool", a region of the Atlantic dominated by swell. Another turning point in the EF can be found approximately at 130°S in the equatorial Pacific.

During winter, the intense storms in the North-Pacific and North-Atlantic generate waves that travel southwards beyond the equator defining two fronts from New Zealand to North-America and from South-America to Africa, from which swell waves from the south-west travel north-easternward (i.e. south-west wave direction). During austral winter, due to the widening and strengthening of the storms in the SH and the weakening in the NH, the swell wave coming from the Southern Ocean dominates these areas provoking large shifts in the time series of EF direction. This behavior is also reflected in the seasonal variations within the tropics (see Figure 3.8).

Also reflected in the standard deviation of the annual signal, the Atlantic basin is characterized by a standard deviation above 135°, covering from the eastern border of South-America to the western limit of Africa, revealing the area where wave directions shift during the corresponding hemispheres winters. From this point to northern Oceania, another border with standard deviation over 135° can be identified. The nearby coasts to this large deviation regions are of concern because changes in energy flux directions are expected to have implications in coastal sediment systems. Considering the study of long-term trends in these areas, special caution must be taking due to the large shifts found which make unfeasible standard regression analysis.

Smaller regions with high deviations can also be found near the coastal areas of the North Atlantic, Caribbean Sea and along the Asian margin. Values of deviation between 15° and 30° are identified, at 30°N in the Pacific, over 30°N in the Atlantic towards North-America and some scattered regions in the SH. In the global ocean, the annual deviation of energy flux direction is below 15° (i.e. low shifts in mean wave energy direction). The directional variability found here is consistent with previous findings in terms of mean direction ([Young, 1999] and [Hemer et al., 2010]).

3.3.3.2 Coastal directional wave climate

As surface ocean waves propagate from the deep water zone towards the coast, they undergo a range of transformations (shoaling, refraction, diffraction, blocking by land, frictional losses

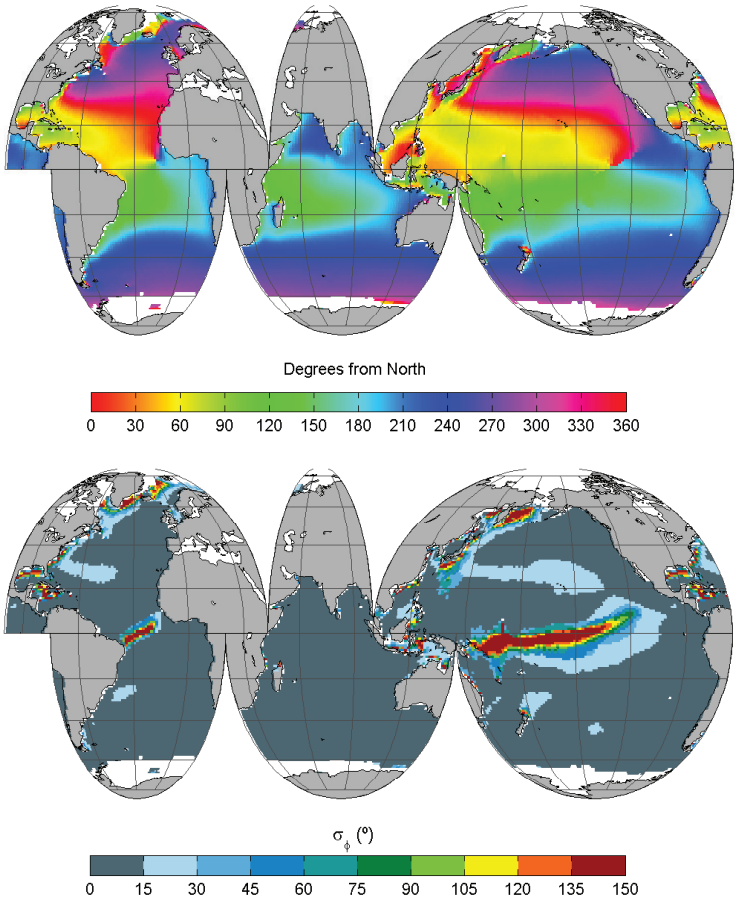

Figure 3.7: Mean annual direction of Energy Flux (in degrees from North).

and scouring at the sea-bed, depth-induced breaking etc). For example, wave refraction make waves turn, tending to approach shore normally. As a consequence, the impact of a changing offshore wave climate is not always experienced at the coast. Some sections of coast may be more sensitive to changes in the offshore wave climate than others. To approximately account for this effect in the wave climate properties, in this section a simple propagation case is addressed based on Snell´s law (on a hourly basis), which relates the change in direction of the waves to the change in wave celerity, and the conservation of energy.

In a steady-state case, where there are not any energy losses or inputs and no energy flux across wave rays, the energy flux at two different points (denoted by 1 and 2) must be conserved. Due to the convergence or divergence of the wave rays, resulting from refraction or physical boundaries, and due to changes in depth, the energy per unit area varies. Assuming no wave reflection, the conservation of energy requires:

$$EF_1 \cdot b_1 = EF_2 \cdot b_2 \tag{3.3}$$

where EF represents the total energy flux per wave per unit width and b_i the length of the orthogonal to the wave rays at the two points. In term of wave heights, the equations can be expressed as:

$$H_2 = H_1 \cdot \sqrt{\frac{c_{g1}}{c_{g2}}} \cdot \sqrt{\frac{\cos\theta_1}{\cos\theta_2}} \tag{3.4}$$

where c_g is the group celerity and θ the wave incidence angle (i.e. direction of the wave fronts), which satisfies the Snell´s law and can be obtained from:

$$\frac{\sin\theta_1}{c_1} = \frac{\sin\theta_2}{c_2} \tag{3.5}$$

representing c_i the wave celerity at each location.

For the definition of the wave climate at 10 m depth, here a coastline with straight and parallel contour depths and linear wave theory is assumed. The annual mean energy flux direction is represented in Figure 3.9 computed over sixty years.

Changes in the direction of wave energy can alter the sediment budget and will have consequences for erosion/accretion rates. Obliquity of waves are a major factor affecting longshore sediment transport. In coastal longshore transport, the wave angle with respect to the coastal alignment is a variable of interest. A global shoreline dataset (coastline in ESRI Data Maps was here used) enables coastal alignment to be determined, and consequently the angle of waves with respect to the coast at each point. A shore normal is determined being perpendicular to the main coastal alignment at several points along the world coastline. Figure 3.10 represents the propagated angle of the mean energy flux and the main alignment orthogonally to the coastline (contour depths are assumed straight and parallel to the coastline). The obliquity of the incident wave energy flux serves as an indicator of possible imbalance in the longshore sediment transport. Whether these variables, along with potential sediment transport, are experimenting long-term changes will be explored later in the work (see subsection 3.5.2).

As a matter of fact, the areas of the world with the highest obliquity between their coastline alignment and the annual mean incident wave energy, and thus subject to potential erosion, are located along the west coast of north America, west Africa, Australia and the Coral sea region.

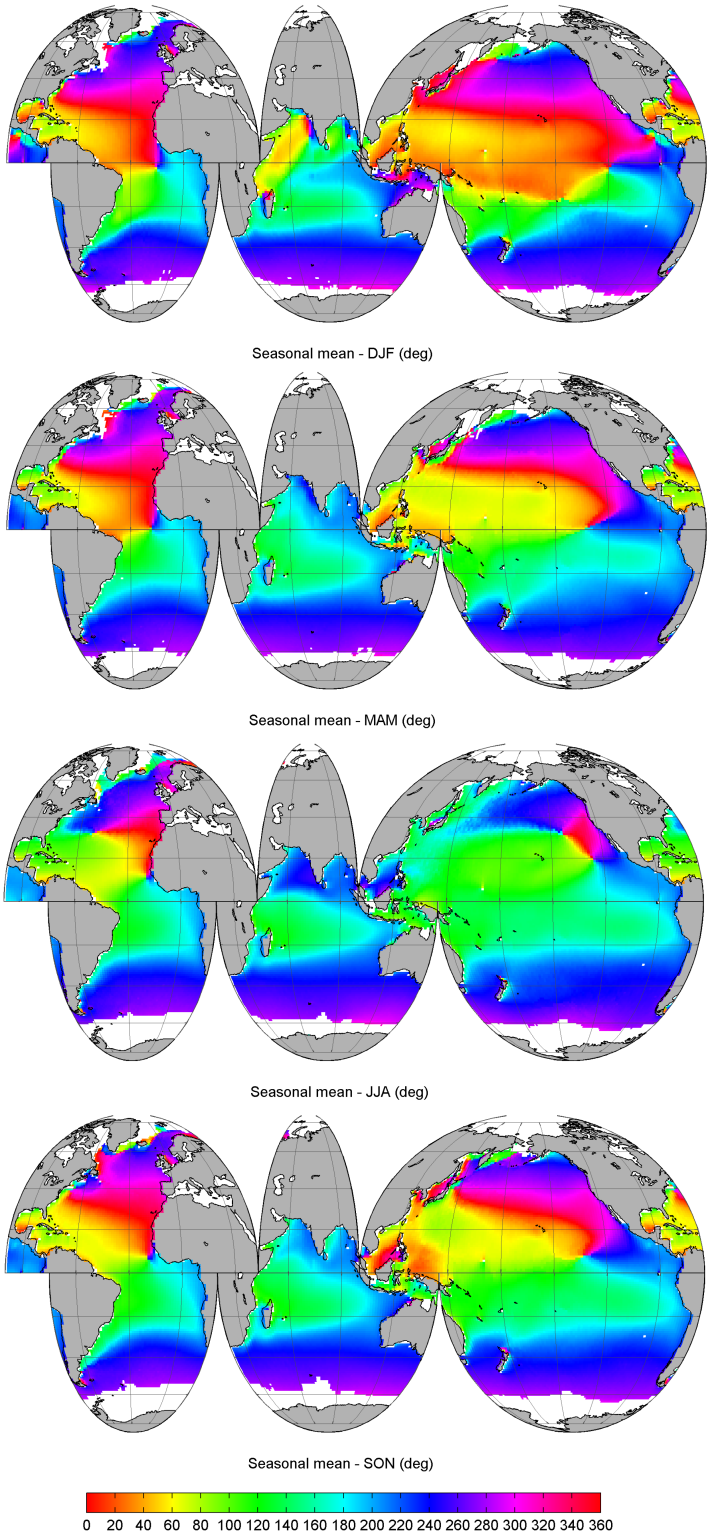

Figure 3.8: Mean direction of seasonal Energy Flux (in degrees from North).

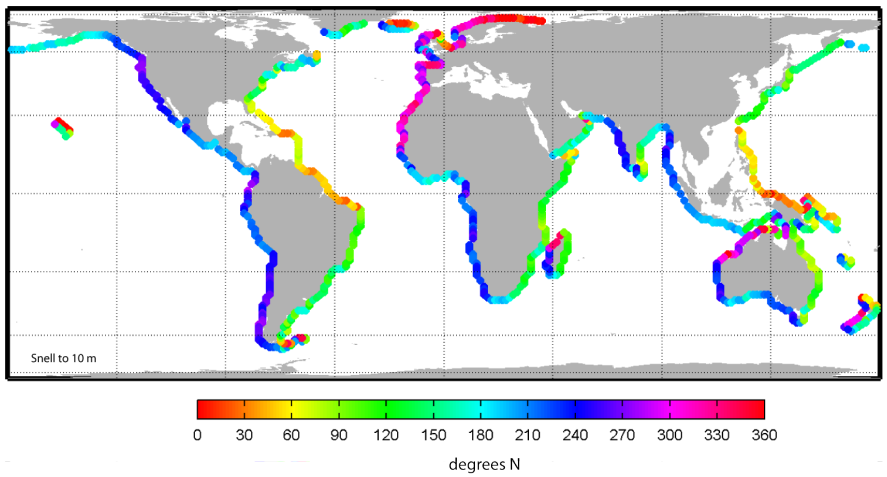

Figure 3.9: Direction of mean energy flux at 10 m depth (propagated by Snell assuming straight and parallel contour depths; expressed in degrees North).

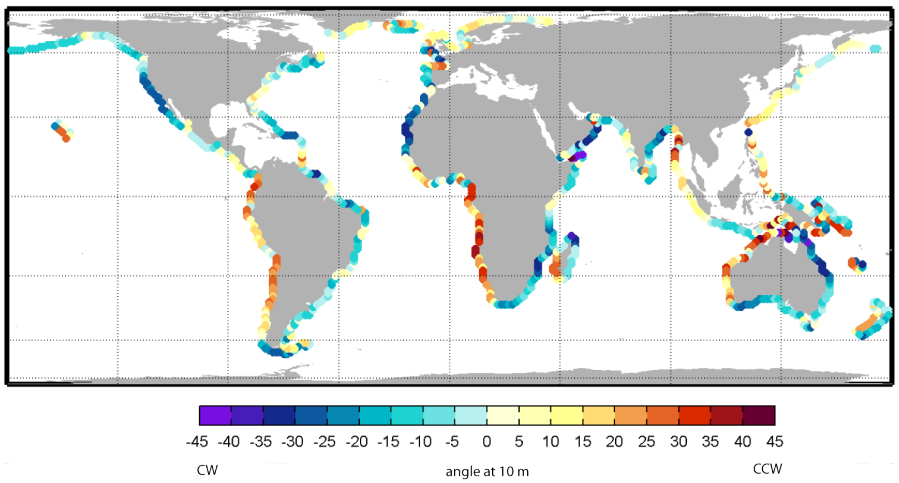

Figure 3.10: Angle between the main alignment of the coast and the annual mean energy flux at 10 m depth computed for the period from 1948 to 2008 (propagated using Snell's law assuming straight and parallel contour depths; expressed in degrees).

3.3.4 Extreme wave climate

Although a high quantile of wave heights have already been described, analysis of previous statistics do not characterize extreme wave climate. A specific approach based on extreme analysis is needed to study wave extremes. This is done by using the Annual Maxima Method on the 61-year wave dataset and fitting a generalized extreme value distribution (GEV) to compute the 100-year return period significant wave height, represented in Figure 3.11.

The spatial pattern here found is consistent with previous works ([Swail and Cox, 2000, Caires and Sterl, 2005a, Izaguirre et al., 2011]). However, results in [Caires and Sterl, 2005a] seem to be larger. This may be associated with the model used for the extreme analysis since [Izaguirre et al., 2011] using a similar approach but different dataset, altimeter data in their case, found heights values that keep a close agreement with those obtained from GOW dataset. This fact is adding evidences that the statistical behavior of the wave reanalysis is well modeled, despite the fact that peaks intensity is not perfectly represented.

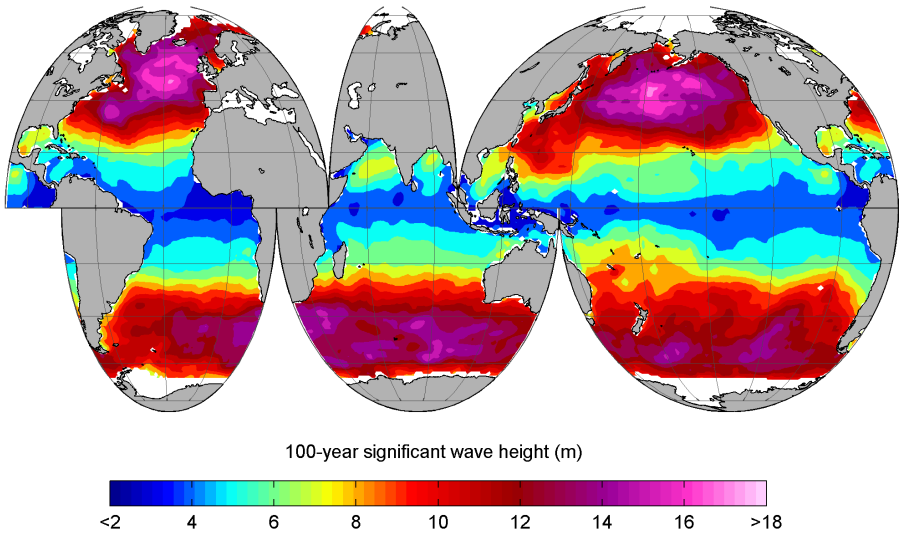

Figure 3.11: 100-year significant wave height (in m), calculated fitting a generalized extreme value distribution to the 61-year maxima values from the dataset (GOW).

As previously pointed out by other authors, the greater range of variability is once more identified in the NH, with the largest wave heights, over 18 m, occurring in the North-Atlantic and North-Pacific, despite being the SH rougher along the year, as proved in previous sections of this work.

3.4 Global wave climate inter-annual variability

Climate variability refers to variations in the mean state and other statistics of the climate on spatial and temporal scales beyond individual weather events ([Solomon et al., 2007]).

Many are the evidences on large climate variations influencing ocean and land systems in the world. [Izaguirre et al., 2011] and other prior studies found relationships between wave extremes and climate patterns. Coastal flooding and coastal erosion has also been related with large climate anomalies (e.g. [Solomon and Forbes, 1999, Andrews et al., 2006, Harley et al., 2010]). During the winter of 1997-98, wind-driven waves and abnormally high sea levels significantly contributed to hundreds of millions of dollars in flood and storm damage in the San Francisco Bay region. Evidences of erosion in Australia with ENSO events has also been reported (e.g. [Ryan et al., 1999, Ranasinghe et al., 2004]). Precipitation is also connected with inter-annual variability (e.g. [Kyte et al., 2006]). Also ecologically, climate patterns seem to influence worldwide. For example, disparate populations and biologically unconnected ecosystems seems to change simultaneously ([Alheit and Bakun, 2010], and citations therein), which indicates that they are most likely responding to ocean basin-scale or global climate variability ([Schwing, 2011]). Additionally, effects of inter-annual variability present a long memory of past events. The impacts of El Niño events, for instance, may be seen in marine systems for several years and its effects on coastal erosion may remain for long or suffer irretrievable reversal.

Climate variations are communicated through fluxes of heat, moisture, and momentum by atmospheric circulation, and via the transport of heat, buoyancy, momentum, and material by the large-scale ocean circulation. The former appear to occur in recognizable patterns of variability via teleconnections ([Horel and Wallace, 1981, Wallace and Gutzler, 1981]). These propagations lead to regional signals that alter the processes in marine ecosystems, climate dynamics and coastal systems. These atmospheric teleconnections create well-defined anomaly patterns in decadal and other climate scales, often summarized by spatial patterns and temporal indices, commonly used as climate indices.

Concerning wave climate, many studies have addressed the study of wave heights inter-annual variability. For example, [Gulev et al., 2001] found that Atlantic cyclone frequency demonstrates a high correlation with the North Atlantic Oscillation (NAO) and [Woolf and Challenor, 2002] also show that this index is strongly correlated with the leading mode of inter-annual variability in monthly mean wave heights in the North Atlantic. Similarly, the SAM index is known as the most influencing pattern in the wave climate in the SH [Hemer et al., 2010]. [Gulev and Grigorieva, 2004] found that the mean H_s in the Pacific is correlated with the El Niño Southern Oscillation (ENSO). The Pacific North-America Index (PNA) is also largely linked to the eastern Pacific cyclone activity over the Gulf region and the North American coast [Gulev et al., 2001]. Some studies have also addressed the directional analysis ([Hemer et al., 2010]), although they are more scarce.

This section addresses the study of the linkage between the global wave climate and some of the most known climate indices. This is mainly done in terms of correlation of monthly time series of several variables, like wave heights and energy direction, with different climate indices.

3.4.1 Inter-annual variability of wave heights

3.4.1.1 Correlation patterns

Prior to see the effect of the most prominent climate indices controlling the wave climate, it is necessary to provide an overview of the global wind circulation and pressure patterns. Figure 3.12 represents both patterns for January and July months, selected as representative of the winter and summer season at each hemisphere. It can be clearly seen the southward shift of the high pressure centers during each winter season and the generation areas associated with the low pressures in each ocean basin. From such a behavior, it would be expected some sort of correspondence between the main wind anomalies and the global wave climate.

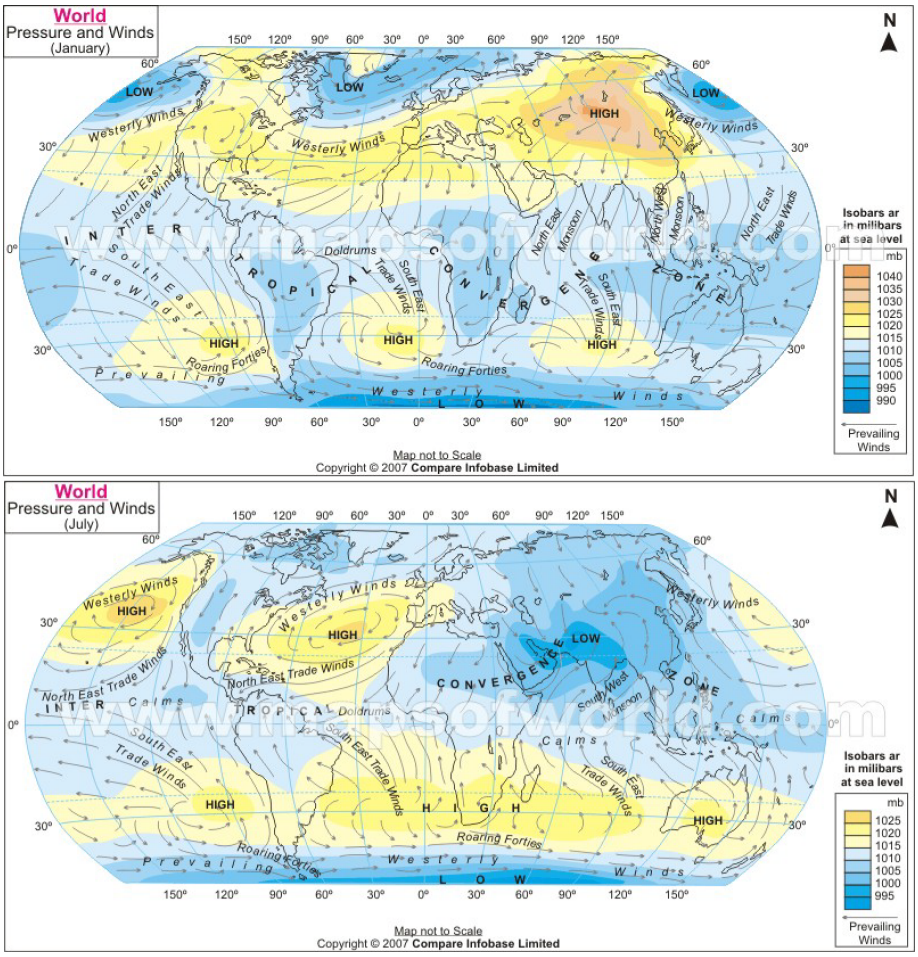

Figure 3.12: Global mean wind circulation and atmospheric pressure pattern for January (upper panel) and July (lower panel). Source: www.mapsofworld.com

Figure 3.15 represents in a mosaic the spatial patterns of the Pearson correlation coefficient, r (ranging from -1 to 1, where 0 is null correlation and ± 1 means total correlation), between the anomaly of the monthly mean H_s and several climate indices.

The most prominent influencing patterns for each hemisphere are the Artic Oscilation (AO) and the Southern Hemisphere Annular Mode (SAM). Figure 3.15 represents the correlation patterns with the monthly mean H_s. The same calculations were computed for the 90^{th} percentile of H_s obtaining similar spatial patterns but some differences appear, generally depicting lower correlation. In the following, each climate pattern description and explanation is given.

Positive phase of AO is related to lower pressures in the Arctic which provokes a shift of the storms northward with an intensification of the westerlies winds. This implies an intensification of the wave heights in the North Atlantic over the 50°N with dominance of the West to North-West directions. The results show that, in terms of correlation with the wave heights, the influence of the AO is widespread in the NH with high positive correlation in the northern border of the North Atlantic, strong negative correlation below 40°N and slightly lower in the Northern Pacific ocean. Other low correlation regions are the northern Indian ocean, west of Guinea Gulf and mid-Atlantic. This climatic pattern is also related with a strong decrease in the wave heights in the Atlantic and moderate in the Pacific, both between the 25 and 40°N. This pattern is also correlated with a decrease in the Southwest Monsoon intensity, as seen in the northern Indian Ocean.

With respect to the SAM mode, a positive phase of the index is associated with a center of low pressure in the South Pole and a ring of high pressure anomalies at mid-latitudes. This leads to a zonal wind anomaly in a broad band around 55°S with stronger westerlies, that provokes a widespread influence in the SH wave heights, in agreement with previous studies (see [Hemer et al., 2010]), and showing positive correlations over 0.5 at high latitudes, negative correlation below 50°S from the Atlantic to the Indian, and small positive correlation along the Coral Sea and the South-East Pacific, affecting the western border of America.

In the Atlantic, the North Atlantic Oscillation (NAO), the Scandinavian index (SCA) and the East Atlantic Pattern (EA) present the strongest influence in the Atlantic wave climate. The NAO pattern consists on a North-South oscillation of the pressure fields. When the NAO index is high, the westerlies are stronger than average which involves an increase of wave heights over 40°N in the Atlantic and a sink around 35°N. The influence of NAO index in the northeast Atlantic can be associated with swell variations [Gulev and Grigorieva, 2006]. Figure 3.15 shows that the NAO index has a significant influence in the North Atlantic showing positive correlations of 0.5 over the 45°N and negative (-0.3) below that latitude. This result is consistent with previous studies such as [Woolf and Challenor, 2002] and [Dodet et al., 2010] who found correlations between 0.1 and 0.5 for the mean H_s in the area. Another positive correlation area extends from 0 to 20°N ($r = 0.2$). Negative correlation (r = -0.15) is revealed in the western and eastern equatorial Atlantic. As occurring with the AO pattern, the linkage with the Southwest Monsoon in the Indian Ocean is also present.

The EA pattern [Barnston and Livezey, 1987] also consists of a North-South of pressure dipole in the Atlantic, in this case spanning from East to West and with the anomaly center displaced southeastward. This pattern provokes a general increase of heights in the East Atlantic reaching the tropical Atlantic with a maximum correlation around the 40°N associated with swells shifting to North-West direction, as previously shown by [Izaguirre et al., 2011] from altimeter observations. EA influences the eastern coast of the Atlantic, from the eastern coast of Europe to the Equator in Africa, with values of Pearson´s correlation coefficient around 0.4. Comparatively,

the SCA index [Barnston and Livezey, 1987] shows a weaker correlation (not shown) and affects mainly the North of Europe because the anomaly center is located at northern Siberia and above the Arctic sea, hence decreasing wave generation in the North Atlantic.

The Tropical Northern Atlantic Index (TNA) is an indicator of the surface temperature in the eastern tropical North Atlantic Ocean and was defined by [Enfield and Mayer, 1997, Penland and Matrosova, 1998]. Positive correlations with wave heights are found broadly in the Pacific and most of the Atlantic with the exception of negative influence in the southwest tropical Atlantic, northern Europe and South Asian coasts. TNA effect is widespread manifest in the Pacific (shown by positive low correlation as a collateral effect) and linked with strong regional features in the Atlantic basin. Positive phases of the index decrease wave heights in the northern and central areas of the Atlantic, while increasing them in the Guinean Gulf and a region between 20 and 40°N.

One of the most prominent modes of low-frequency variability in the Northern Hemisphere that affects the Pacific Ocean is the Pacific North American pattern (PNA). The PNA pattern is associated with strong fluctuations in the strength and location of the East Asian jet stream and with an eastward shift in the jet exit region toward western North-America. In terms of wave heights, these winds indicate an increase in wave heights in the North-Pacific, extending their effect to the 25°S, reaching the Peruvian coasts. Negative lower correlations, associated with a decrease in the wave heights are found in the tropical southwest Atlantic and southwest Pacific.

Finally, the Western Pacific index (WP), described by [Barnston and Livezey, 1987, Wallace and Gutzler, 1981], consists of a north-south dipole of anomalies with one center over the Kamchatka Peninsula and another broad center of opposite sign located over southeastern Asia and the western south tropical Pacific. This climate pattern (correlation pattern not shown) modifies the East Asian jet stream provoking a dampening of wave heights between the 25 and 50°N and an increase outside that particular latitude band, which is specially remarkable at the east of the mentioned peninsula. Other teleconnections with negative phase of this index are found in the North tropical Atlantic and south Indian Ocean.

Another climate pattern affecting wave heights in the Pacific is the East Pacific - North Pacific pattern (EP-NP) which presents three main anomaly centers, the positive phase featuring positive anomalies over Alaska and Western Canada, and negative anomalies over the central north Pacific and eastern North-America. Positive phases are associated with a southward shift and an intensification of the Pacific jet stream from eastern Asia to the eastern North Pacific which generates waves from east to west in the North Pacific and heavily decrease the wave heights, reaching the western coast of America, from north to south. Weaker influences are found along particular areas of the Atlantic and the Indian Ocean, generally close to the coastline.

Two climate indices representative of the Indian Ocean has been studied, the Indian Ocean Dipole (IOD; [Saji et al., 1999]), measured through the Dipole Mode Index (DMI), and the Quasi-Biennial Oscillation (QBO) also known as Singapore Winds (not shown). The correlation analysis reveals a decrease in heights in the mid Indian Ocean and a weak linkage in the south Pacific with positive phases of the index. Weak positive influence is found along several regions of the Pacific and the south Atlantic and Indian Oceans.

Correlation with the Atlantic multidecadal Oscillation (AMO) index (not shown) shows a positive influence in the mid-Pacific (r over 0.2) affecting the whole American western margin. A slightly negative center of correlation is detected at the north-west of this basin reaching the northern coast of Japan. A second striking region is found in the South-Atlantic, with remarkable positive correlation (r over 0.4) in the Guinean Gulf. Secondary centers are found at mid Atlantic, from the equator to 20°N (correlation values below -0.25), North Atlantic and Northern sea. In the Southern Ocean a weak positive correlation is detected as well (r below +0.2).

El Niño-Southern Oscillation (ENSO) cycle refers to variations in the temperature of the surface of the tropical eastern Pacific Ocean (warming and cooling known as El Niño and La Niña respectively) and in air surface pressure in the tropical western Pacific ([Dijkstra, 2006]). The ENSO cycle is the most prominent year-to-year climate variation on Earth, and is also reflected in the wave climate. El-Niño and La-Niña typically recur every 2 to 7 years and develop in association with swings in the Southern Oscillation, intimately related to the strength of the Pacific trade winds (Figure 3.13). During El Niño positive phase (or conversely negative SOI index), the trade winds weaken along the equator as atmospheric pressure rises in the western Pacific and falls in the eastern Pacific. Anomalous warming in the central and eastern Pacific ensues as warm water in the western Pacific migrates eastward and upwelling is reduced. These changes are commonly linked to changes in the latitude and longitudinal extent of the Pacific storm track ([Seager et al., 2003, Seager et al., 2010]) as represented in Figure 3.14. During El-Niño winters (i.e. negative SOI) the storm track tends to maintain an eastward route from the central Pacific and head into southwestern North America while, during La-Niña winters, the northeastward deflection over the eastern Pacific is exaggerated. These changes in the storm track are fundamental to understand its effect on the wave climate.

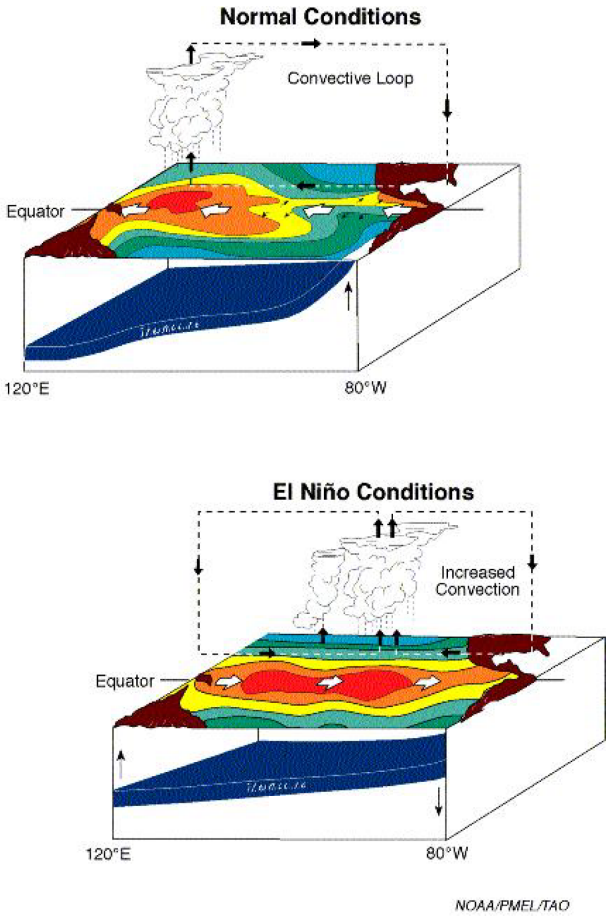

Figure 3.13: The Walker circulation in the atmosphere and the position of the thermocline in the ocean in normal conditions and in El Niño years. Red represents warm SST while green ones represents cold water. Source: NOAA.)

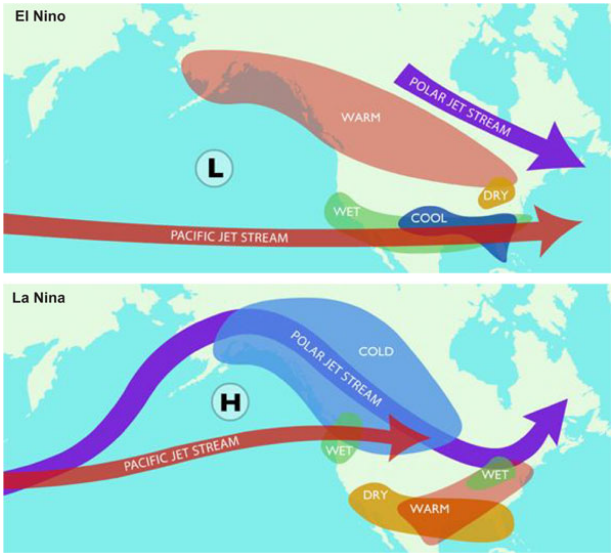

Figure 3.14: El Niño and La Niña climate patterns in the North Pacific. Credit: Smithsonian Institution.

The Southern Oscillation, whose strength is measured by the Southern Oscillation Index (SOI), is the atmospheric component of El-Niño, and consists of an irregular strengthening and weakening of the trade winds. Analogously, the Niño3 index is an average of the sea surface temperatures in the region 150-90 °W and 5°N to 5°S. The ENSO phenomenon identified by those two indices (correlation pattern for Niño3 not shown) reflects a positive low correlation (r from -0.2 to -0.3) in the Pacific ocean (north and tropical west), reaching a positive value of 0.3 at South-America border extending its influence westernward, because of a twofold effect: (1) weakening of trade winds and (2) southward shift of storm tracks in the northern Pacific. These results are consistent with those in [Hemer et al., 2010] for the SH.

3.4.1.2 Mean contribution to wave climate

Through a simple regression analysis, the mean contribution per unit of standardized climate index can be easily obtained. This contribution to wave heights varies throughout the year as does the mean and variance of wave heights for each month. Whether this effect can be important for global wave climate is explored below.

Figures 3.16 and 3.17 show this contribution for the 90^{th} percentile of H_s in two months of the year, December and June, expressed in meters of wave height and as a percentage of the mean monthly conditions of the wave statistics. This double representation aims at identifying not only the largest contribution to wave heights but also the areas where climate variability may be playing an important role in the wave climate, despite its roughness.

Each unit of standardized index of PNA explains about 0.6 m in the North-Pacific and 0.2 m along the coast of the North-American coast. However, during the summer the contribution decreases, but the effect is maintained in proportion, being responsible of between a 5 and 10 % in the north-east Pacific all year round, due to a reduction of both the index influence and the wave heights.

In the case of AMO index, it explains over 0.6 m both in December and June in large parts of the SH, and about 0.2 m in the South-Atlantic which particularly corresponds to a high percentage of the mean conditions for the area. The contribution strengthens during winter in the North-Pacific and North-Atlantic due to higher storm activity, while in the SH it represents a higher proportion of its wave climate as the storm area gets narrower, previously shown in this work.

3.4.2 Inter-annual variability of mean energy flux direction

The study of links of climate indices with different wave heights statistics has been traditionally studied more deeply than the EF direction. However, the variability of wave directions is essential in defining the influence of a changing wave climate on the coastal zones. Changes in the wave directions can alter the longshore sediment transport due to wave-driven currents variations. Sand transport in coastal zone are dominated by wave-driven currents, whose strength and direction are wave direction dependent [Longuet-Higgins, 1970]. For example, changes have been observed [Masselink and Pattiaratchi, 2001, Harvey, 1996, Hou et al., 2003] in longshore

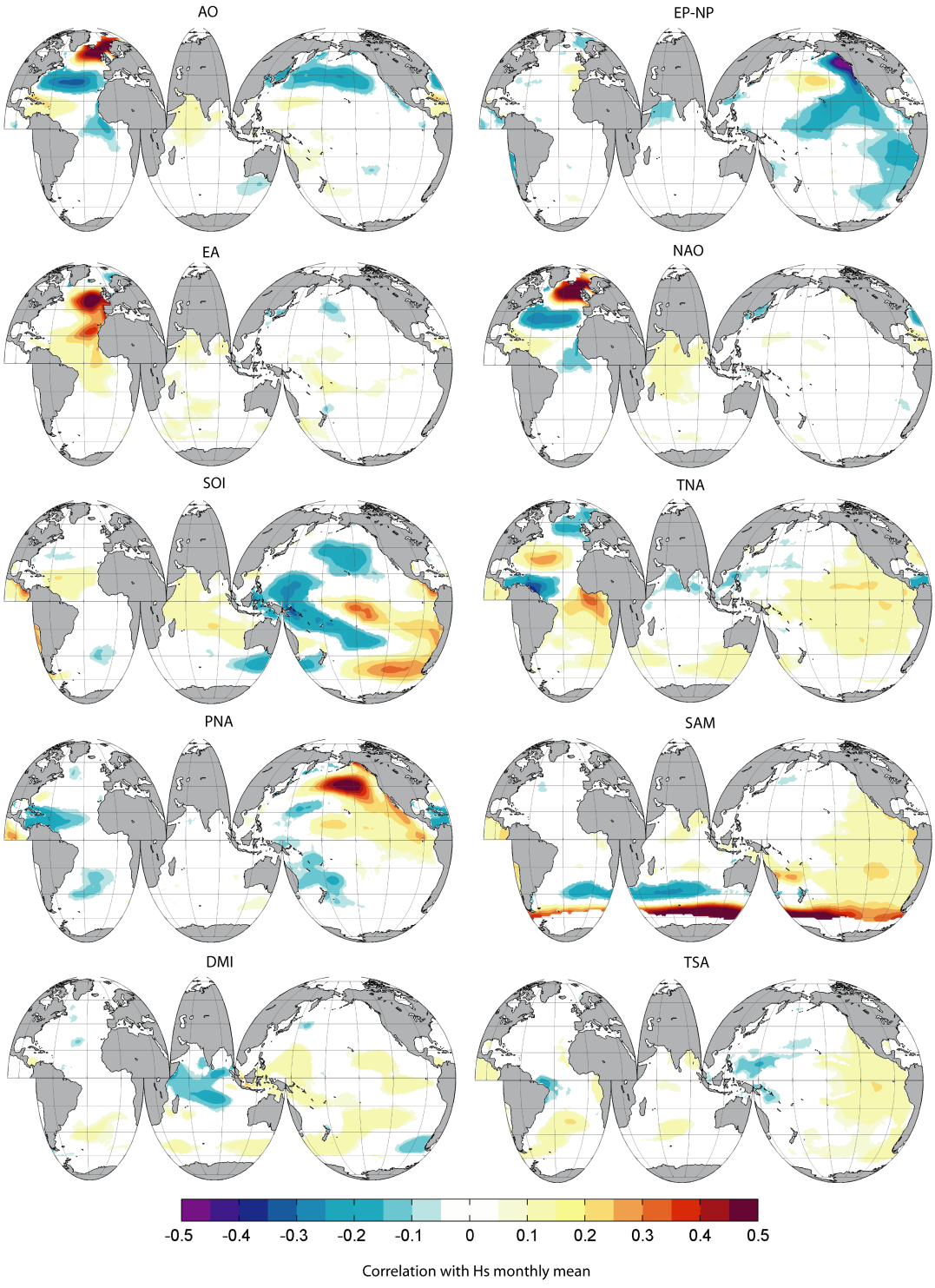

Figure 3.15: Correlation of several climate indices with monthly standardized anomaly of the mean significant wave height (using Pearson´s correlation coefficient.)

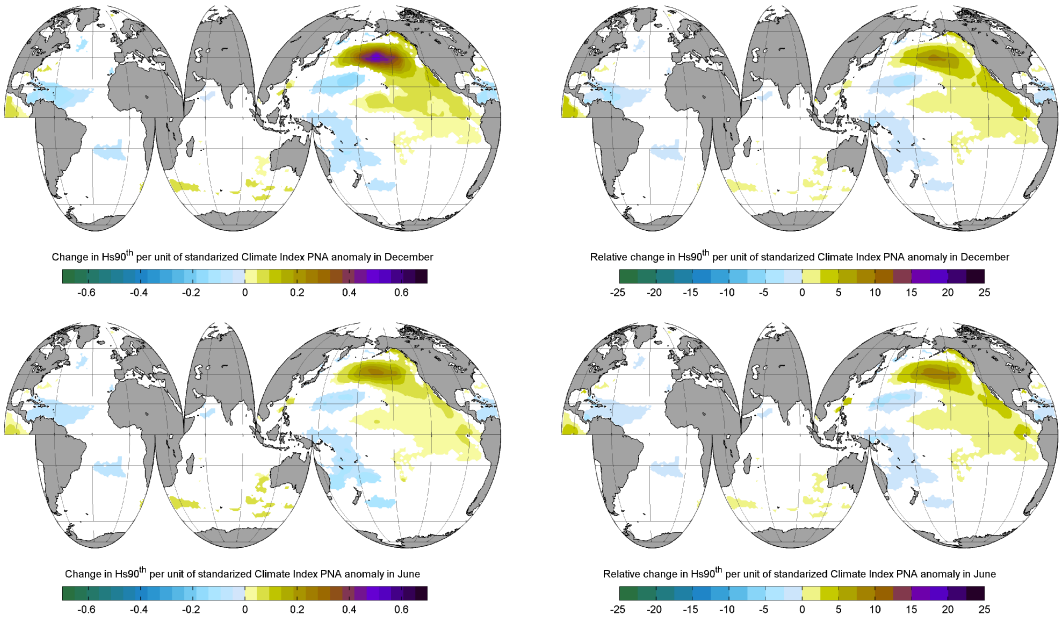

Figure 3.16: Contribution of 90^{th} percentile to significant wave height per unit of standardized PNA index for December (upper panels) and June (lower panels) expressed in meters (left panels) and as a percentage of monthly mean conditions (right panels).

transport along western Australian coast margin due to an incident wave direction rotation. Also [Hepner and Davis, 2004] show that El-Niño weather pattern has a major influence on the beaches of the Florida peninsula due to derived changes in littoral sediment transport and also in Australia, provoking beach rotation [Ranasinghe et al., 2004, Harley et al., 2010]. Moreover, [Hemer et al., 2010] cite that directional variability of wave energy flux in the western Pacific Ocean has been shown to affect importantly the sand transport along the south-eastern Australian and New Zealand regions. They studied the variability and trends of directional wave climate from C-ERA-40 reanalysis for the period 1958-2001 and found a clockwise rotation of flux vectors in the western Pacific during El-Niño events.

Here, this variability is explored on a global scale and for many of the most extended climate patterns in the global climate system. The analysis is based on the correlation of the monthly anomaly (i.e. with respect to the monthly mean) of the EF direction (in degrees) with the climate indices representing the climate patterns. This is a novel step since the unique analysis based on the study of the EF direction to date, [Hemer et al., 2010], was made in vectorial components. Computing the analysis for angle anomaly instead represents the shift in the wave energy quantitatively better. As a consequence, a better understanding of changes and their implications is possible.

Mean EF direction patterns greatly differ with wave heights correlation results. Figure 3.18 displays the correlation patterns obtained for the mean EF direction. Some correlation patterns are particularly noteworthy representing great shifts in some ocean basins. The Southern Ocean

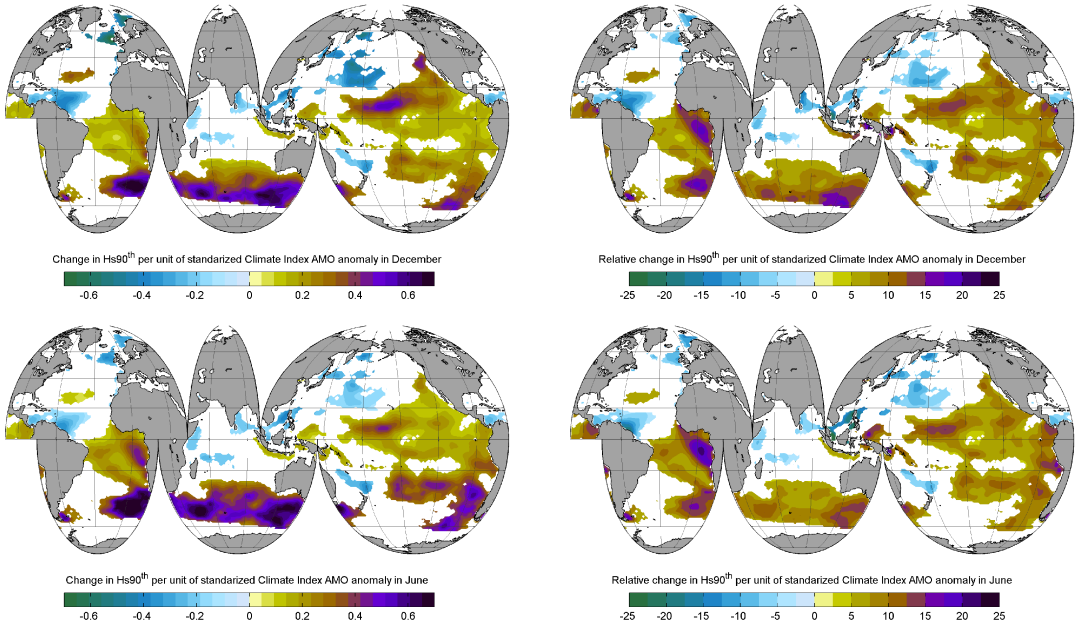

Figure 3.17: Contribution of 90^{th} percentile to significant wave height per unit of standardized AMO index for December (upper panels) and June (lower panels) expressed in meters (left panels) and as a percentage of monthly mean conditions (right panels)).

is clearly affected by SAM pattern (consistent with findings in [Hemer et al., 2010]), while the North Atlantic is controlled by AO and NAO. In the Pacific the dominance of PNA and EP-NP is clear.

A positive anomaly of SAM is associated with a counter-clockwise rotation along all the Southern ocean with a great negative correlation (r over 0.5) at the southern Indian border, reaching western Australia territory. Additionally, regional features affect the South-Atlantic and Pacific oceans.

Key regions with wave direction shifts are present in all ocean basins. In the Atlantic ocean, AO and NAO are the patterns that mainly control the mean EF direction anomaly. AO provokes a clockwise rotation from 0 to 30°N in the North-Atlantic, while a counter-clockwise rotation affects the North Sea, north-western area and the Guinean Gulf. The NAO pattern keeps great similarities with AO but differs in the appearance of a counter-clockwise rotation closer to European coasts instead of the north-west rotation center. North Sea and tropical Atlantic are still affected by the counter and clockwise rotation, respectively. TNA also shows a counter-clockwise shift around the 20°N latitudinal band. Regional features affecting the south Atlantic are also associated with this index with two remarkable centers of counter-clockwise change at 20°S and the Guinean Gulf.

With respect to the Pacific Ocean, it is mainly affected by PNA and EP-NP patterns. These indices provoke counter-clockwise rotations of mean direction of wave energy at two prominent regions located one at the northern margin of the basin and another centered in the basin at 20°N. Two differentiating features are that PNA presents a greater correlation in the northern area and its influence extends to the equator. No significant influence is found in the South-Pacific for the EP-NP index. However, PNA does induce a shift counter-clockwise at the eastern margin, affecting the equatorial American coast. SOI is the third pattern in importance affecting the Pacific basin. Two areas of counter-clockwise rotation affect the western area (coast of Asia) and South-America southwards from 20°N. A secondary center of rotation, in this case in the clockwise sense, is located in the North-Pacific and seems to affect the North-America western coast. The negative correlation centered in the west reaches Australian south-eastern coast. This means that in the Tasman Sea an El Niño event is associated (i.e. negative anomaly of SOI index) with a clockwise rotation of the wave EF, consistent with [Goodwin, 2005] and [Hemer et al., 2010]. SAM also implies a counter-clockwise rotation in the southern Pacific (in agreement with [Hemer et al., 2010] results) affecting western coasts of Australia and a secondary center of positive sign in the tropical south Pacific. Finally, the DMI index shows correlation at the west-equatorial Pacific, therefore provoking waves shifting southwardly.

SOI and DMI control wave climate direction in the Indian Ocean. Positive phases of DMI index are linked with a counter-clockwise shift in the north-eastern margin of the basin affecting coasts in south India and Indonesia. On the contrary, SOI makes waves shift clockwisely in the same region but its influence is extended to Timor and Arafura seas. Not only the eastern margin of Australia is affected by SOI but also the western coast suffers of a clockwise shift in wave direction under El Niño events (negative SOI anomaly) from 20 to 40°S.

Directional shifts in the Tasman Sea wave parameters have been related with SOI [Short et al., 1995a, Short et al., 1995b, Ranasinghe et al., 2004, Goodwin, 2005].

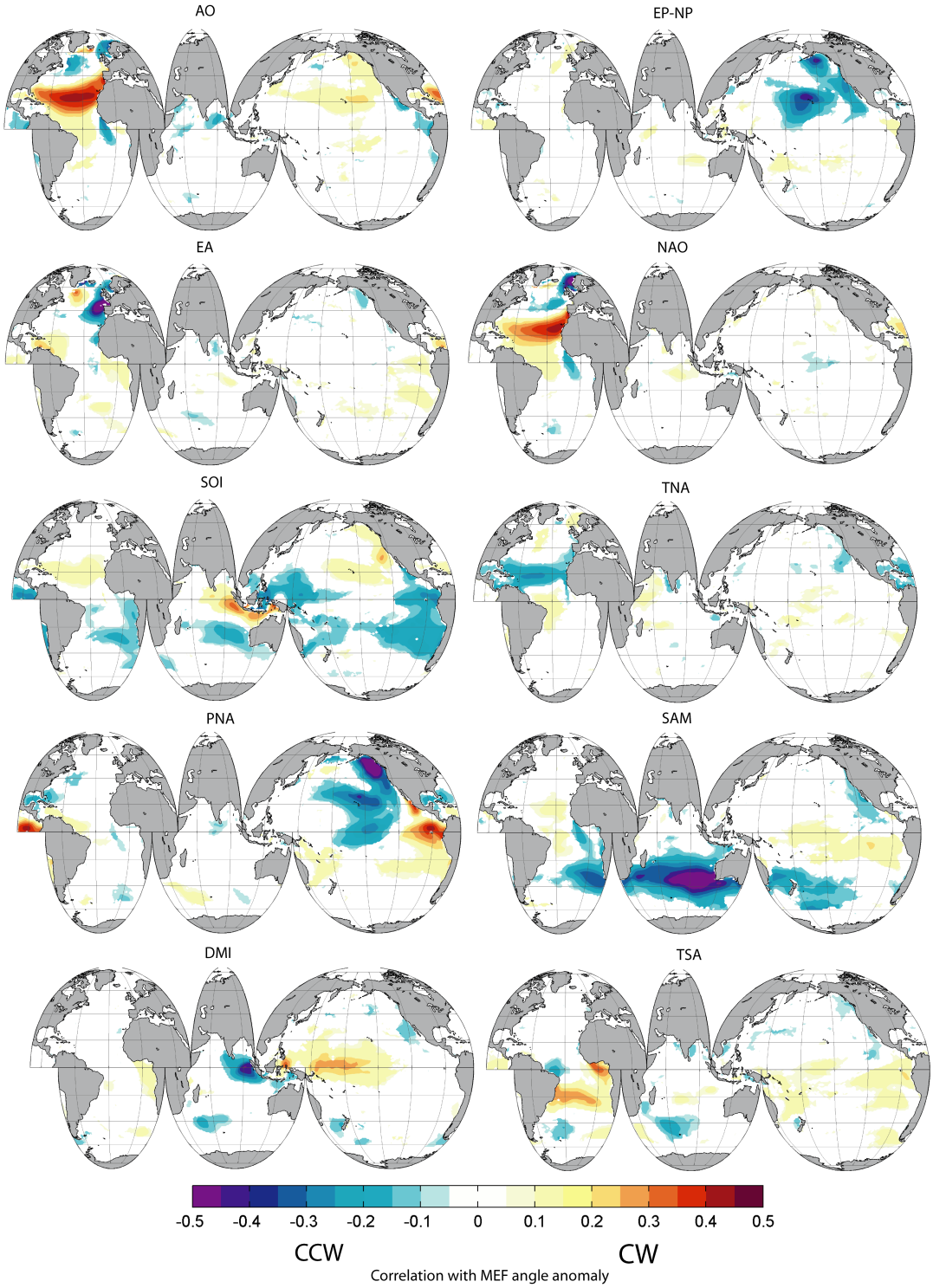

Figure 3.18: Correlation of several climate indices with monthly standardized anomaly of the mean energy flux direction, using Pearson´s correlation coefficient. CCW denotes counterclockwise shift and CW clockwise shift.

[Hemer et al., 2010] finds significant correlations between this index and the eastward EF component throughout most of the Pacific Ocean, while the northward component shows correlation during spring and summer months. Our results for SAM and SOI indices were qualitatively compared with results in [Hemer et al., 2010] using mean EF eastwards and northwards components (instead of angle anomaly), resulting in a great concordance between both studies. Note that in our case, we aim at studying the angle anomaly instead of the mean EF components because it is a more meaningful information for coastal impacts and derived consequences.

Because mean EF direction is closely related with beach planform erosion the variability here presented may be helpful to explain observed erosion/accretion patterns. [Ranasinghe et al., 2004] notice that the northern end of New South Wales beaches accretes during positive El-Niño phases (i.e. negative SOI phases). From our results, negative SOI implies a clockwise rotation of mean EF direction (of opposite sign in Figure 3.18) which agrees with beach erosion observations in the region.

3.5 Long-term changes in global wave climate

Numerous evidences suggest long-term changes in the intensity and frequency of storms (e.g. [McCabe et al., 2001, Gulev et al., 2001, Wang et al., 2006, Ulbrich et al., 2009, Alexandersson et al., 2000, Bengtsson et al., 2006, Leckebusch et al., 2006, Pinto et al., 2007, Wang et al., 2011] characterized by a decrease in activity in the mid-latitudes and an increase in the high latitudes on the NH.

Detection of long-term trends is conditioned within other factors by the time span of available data ([Weatherhead et al., 1998]). Over the oceans, visual observations of waves have been used to assess historical trends ([Gulev and Grigorieva, 2004, Gulev and Grigorieva, 2006]). Buoy measurements are available only in few locations and with only a few decades coverage. Satellite altimeter observations are available in a global scale but their temporal coverage spans from 1985 onwards ([Young, 1999, Young et al., 2011]). Consequently, global wave hindcasts driven by reanalyzed wind fields with long time span are particularly attractive to address this issue, notwithstanding some precautions must be taken.

In this section, the study of long-term changes in global wave climate is addressed. Trends in wave heights, mean EF direction and extreme events are explored based on GOW wave reanalysis dataset and different statistical techniques.

3.5.1 Long-term changes in wave heights

Many studies have analyzed measured or reanalyzed data to detect trends of change in past wave climatology. Studies based on wave hindcasts [Group, 1998, Cox and Swail, 2001, Wang and Swail, 2002, Sterl and Caires, 2005, Hemer et al., 2010, Dodet et al., 2010] based on NCEP-NCAR or ERA-40 reanalysis winds have shown a growing mean H_s as well as an intensification of the extremes during the last four decades of the last century. In the northeast Atlantic

in particular, the 99% extreme of the winter H_s increased by a maximum of 40 cm per decade [Wang and Swail, 2001, Caires and Sterl, 2005a]. In the northeast Pacific, buoy records report growing H_s for the period 1978-1999 [Allan and Komar, 2000, Gower, 2002] with increasing values from 1.2 to 2.7 cm/yr, also reflected in the extremes [Menendez et al., 2008]. The results to be presented here are also consistent with those findings.

In the present work, long-term changes are derived from the GOW dataset for the period 1948-2008. The trends are quantified as a linear function over the duration of the time series and the statistical significance is checked using a Student´s t-test. Given the wave reanalysis spatial resolution, each trend result is representative of a 1.5°x1.0° region.

The results of the analysis of the linear trends of H_s (Figure 3.19) show that the largest upward trend coincide with the extratropical storm-track area with a maximum increase in the SH, located in the South-Atlantic and South-Indian oceans, and trends ranging from 1 to 2 cm/yr, as occurring in the NH at the North Pacific and North Atlantic over the 40°N. In the Indian Ocean, the trend is significantly positive below 1cm/yr. However, there is a consistent region, centered in the mid-Pacific, where the mean wave heights are decreasing about 1 cm/yr. The Polynesian area also exhibits a negative trend, below 1cm/yr. Most of the tropical region shows neutral or non significant trends.

Sea and swell components are not discriminated in this analysis, although some studies found differences in trend behavior for these two components ([Gulev and Grigorieva, 2004, Gulev and Grigorieva, 2006]). Based on visual wave observations, [Gulev and Grigorieva, 2004, Gulev and Grigorieva, 2006] found a strong upward trend (from 1 to 2 cm/yr) in the annual and winter H_s in the northwest Atlantic and the northeast Pacific for the period 1958-2002. In the northeast Pacific, buoy records report growing H_s for the period 1978-1999 [Allan and Komar, 2000, Gower, 2002] with increasing values from 1.2 to 2.7 cm/yr, also reflected in the extremes by [Menendez et al., 2008]. Based on reanalyzed data, [Semedo et al., 2011b] also found significant trends in the same range of values. By comparing qualitatively with these results, we find similar patterns in the North-Pacific and North-Atlantic in winter for the H_s.

The 90^{th} percentile of H_s is also analyzed as an indicator of the high tail of the wave height distribution. The spatial pattern of the trend (see Figure 3.20) is very similar to the one previously obtained for the mean H_s. The spatial structure mostly coincides but showing a strong intensification of the trend in general terms. The positive trends in the Southern Ocean exhibit changes about 2 cm/yr and reach over 2.5 cm/yr at the South of New Zealand. A negative trend center is also found in the mid-Pacific with larger changes than in the mean conditions. The northern Pacific Ocean presents again a widespread positive trend around 1 cm/yr but, this time, a maximum over 1.5 in the north-west margin appears not to have been identified for the mean H_s changes. Another negative trend is found in Indonesia region with similar values as for mean H_s. The Indian Ocean pattern of change is generally positive and similar to the mean H_s. A small area of weak change can be found south of Madagascar but it is not remarkable either in intensity nor in extension.

The North-Atlantic is a region that has been extensively studied ([Bacon and Carter, 1991, Group, 1998, Wang and Swail, 2001, Wang et al., 2006, Wang et al., 2009, Dodet et al., 2010]) and therefore suitable for comparison. The North-east Atlantic has been found to have roughened

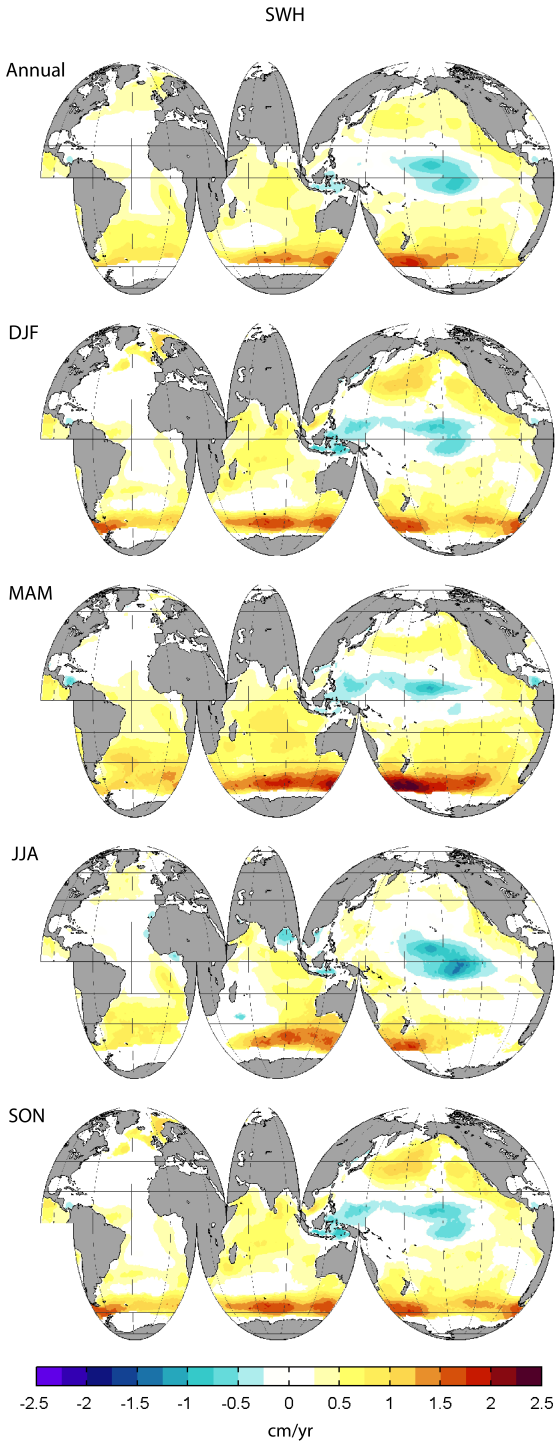

Figure 3.19: Annual and seasonal long-term trends in the significant wave height (cm/yr) in the period from 1948 to 2008, derived from GOW wave database.

in winter during the second part of the last century ([Wang et al., 2009]). A significant decrease in wave heights is also identified in the subtropical area. [Dodet et al., 2010] finds a decrease of 2 cm/yr in the annual 90^{th} percentile of H_s, decreasing southwardly until 40°N after which no significant change is detected. Trends found by [Wang and Swail, 2002] in the same area for the period 1958-1997 display changes between 1 and 2 cm/yr at open waters for the 90^th percentile in winter (i.e. season JFM), matched by significant decreases (1 to 3 cm/yr) in the subtropical North-Atlantic. This dampening in wave heights is found not to be significant here in general terms, though a small significant center of decrease is found for spring (MAM). Qualitatively, the present analysis shows a similar spatial pattern to other studies, with changes about 2 cm/yr in winter.

The Atlantic Ocean shows more changes when comparing with the H_s pattern of change. A positive trend from 1.5 to 2 cm/yr, centered near the South American margin, is found in the southern basin for the 90^{th} percentile, not detected for the mean values. In the North Atlantic, not significant changes are found for this percentile except for the northern limit. These results are consistent with previous findings.

A comparison in mean wave height and 90^{th} percentile is made with the trends obtained by using altimeter observations and reanalysis in the common period from 1992 to 2008. Data from reanalysis were interpolated in time and space to coincide with altimeter observations. Long-term trends have been calculated subsequently. Figure 3.21 displays the spatial pattern of change showing an acceptable agreement with altimeter based patterns in the NH. However, in the SH the discrepancies are notorious, especially for the southern Pacific. These results keep a close agreement with those in [Young et al., 2011].

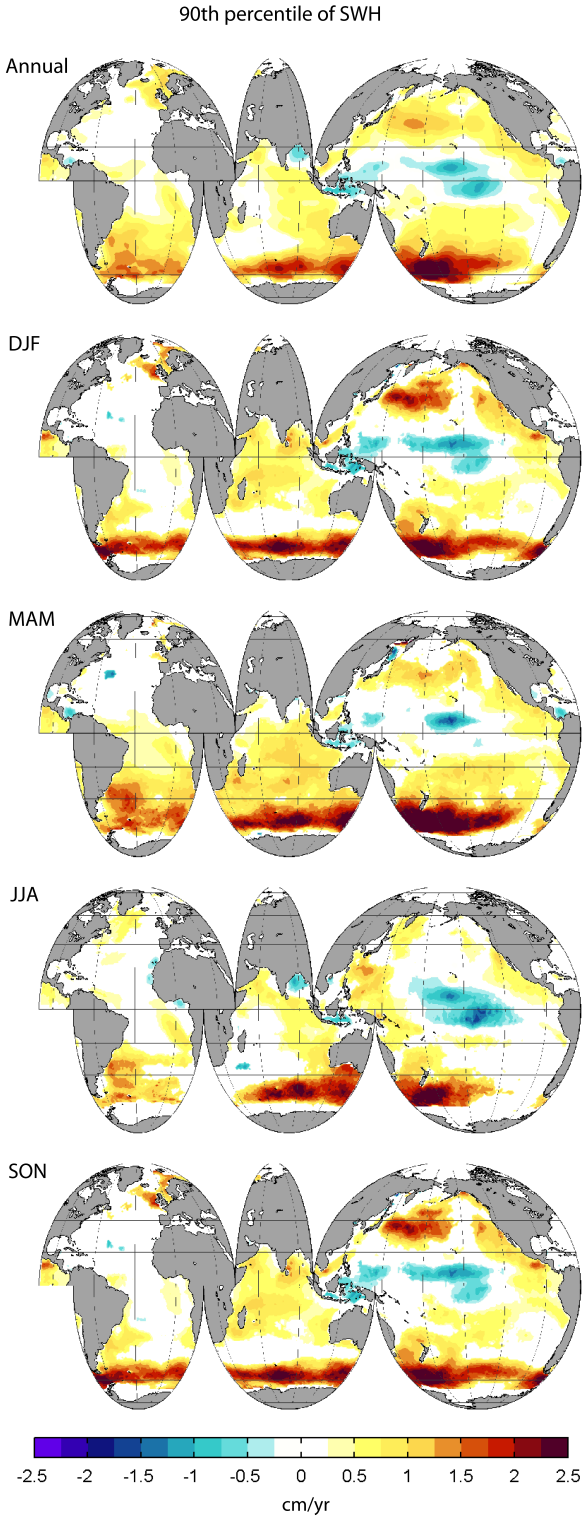

Figure 3.20: Annual and seasonal long-term trends in the 90^{th} percentile of significant wave height (cm/yr) in the period from 1948 to 2008, derived from GOW wave database.

The comparison with long-term trends reveals that the spatial pattern differs significantly from the pattern obtained in the period with altimeter data (Figure 3.21) when considering the 61-years time history. This finding indicates that different patterns of change are identified depending on the time span of available data considered. [Young et al., 2011] point out that it is not possible to distinguish between a sustained trend or a portion of a multidecadal oscillation because the altimeter dataset only covers two decades. They also notice that a longer dataset will be able to separate these possibilities. We consider that the GOW database overcomes these difficulties considering the time history covered. However, a question on the homogeneity of the reanalysis in the SH and whether the trends are representative is still open.

[Hemer et al., 2010] found that the spatial distribution of the altimeter-measured trends are consistent with the C-ERA-40 dataset. However, they found that the numerical based trends overestimate the SH when compared with the altimeter-measured trends. They also confirm that the lower altimeter data are not owed to the sparse sampling of the satellites. In both cases, they found a significant increase in the Southern Ocean wave heights around 45°S, also detected in the eastern Pacific and Indian Oceans, with local wave generation but subject to swell propagation.

These remarks and the present results further supports the difficulty of detecting trends and the aggregate value of numerical reanalysis for their study.

With respect to future climate projections, some studies have carried out dynamic simulations ([Hemer et al., 2006, Mori et al., 2010, Semedo et al., 2011a]). These studies show an increase in wave heights due to increasing wind speeds that are associated with storms in many regions of the mid-latitudes oceans. [Semedo et al., 2011b] have recently developed a dynamical global wave climate projection analyzing differences between present and future global wave climate based on a global circulation model (ECHAM5). The main conclusions from dynamical wave modeling studies are that the largest changes are to be expected at mid to high latitudes, mainly associated with ice coverage (i.e. modification of fetch in generation areas) and changes in the mid-latitude storm tracks. Results in dynamic projections are spatially consistent with patterns of change identified in this work. [Semedo et al., 2011a] find differences between future and present between 0.4 and 0.6 m in the Southern Ocean for annual H_s for the end of the century, and over 0.6 m for the winter wave heights. However, extrapolation of trends here computed would overestimate values with respect to projections, according to such figures.

In general terms, it can be concluded that not only the mean values are increasing but also the high tail of the wave height distribution. Moreover, trends for the 90^{th} percentile are more intense than for the mean value of H_s, coinciding at the same time with lower correlation with climate indices. However, there are regions of the Oceans where extreme values are increasing and mean conditions are not, like in the southern Atlantic or northwestern Pacific. Differences are also identified in the North Atlantic where significant changes are obtained at the northern area.

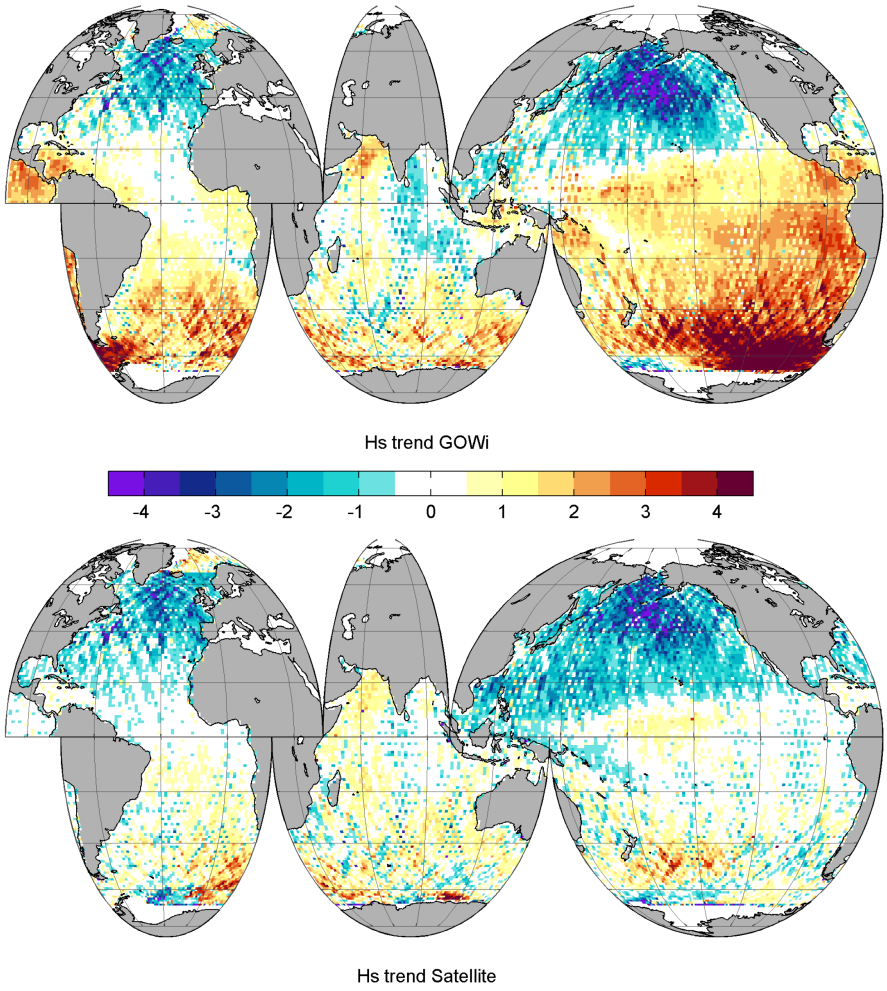

Figure 3.21: Long-term trends for mean annual significant wave height from the satellite altimeter data (lower panel) and from the interpolated GOW data for the same positions and time, for the period from 1992 to 2008 (in cm/yr).

3.5.2 Long-term changes in mean direction of energy flux

The computation of long-term trends for the mean direction of EF is not a simple task. Directional variables present the main disadvantage of representing angles in a circle where 360 and 0 degrees coincide so that the analysis of the data must be done with special caution. Basic linear regression is not appropriate to obtain trends for circular variables because when computing the anomaly over the circle for a certain year, two possible options can be considered. The choice of the right one must be considered inside the regression itself. This has been solved through a specific circular regression analysis explained in detail in chapter 3. Here, results of this method are shown.

Figure 3.22 represents long-term trends and data of the mean direction of EF for five points at certain locations of the global ocean. Directions are represented in a cylinder where the z-axis corresponds to time. The regression model is also displayed with the 90% confident bounds for the data and the regression line, computed as explained in A.2.2. The variability in the time series is notorious in the points at swell pools (point 1 and 4). The directions are maintained in time for the North Atlantic (see point 3). The remaining points show significant trends.

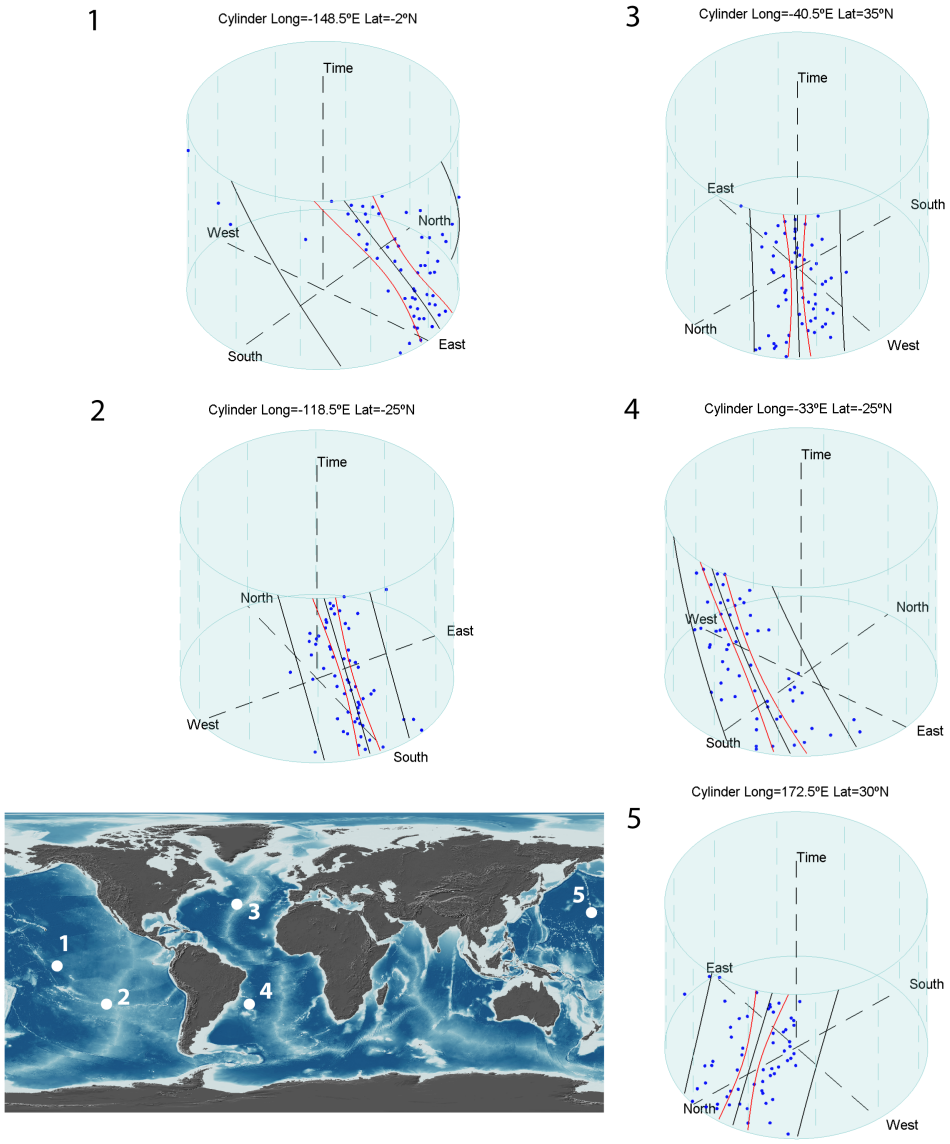

Figure 3.22: Annual long-term trends in energy flux mean direction at five representative points showing the cylindrical evolution and regression with time, for the period from 1948 to 2008. Data have been obtained from GOW wave database.

Long-term trends (a coefficient in the circular regression model) are represented in Figure 3.23. Only statistical significant changes are represented.

Greater shifts seem to be occurring in the mid Pacific with changes of more than 1 degree/yr. Sustained changes in the storm activity in both hemispheres are inducing large shifts of the mean EF direction in the clockwise direction in the South and counter-clockwisely in the North.

Since a discontinuity in trend estimation due to the method seems to exist, a transect in latitude is represented in Figure 3.24 to illustrate that there is no such a discontinuity. Wave climatology results show that the energy flux is highly variable and as a consequence, the westernward shift detected in the trends seems to be a spurious result.

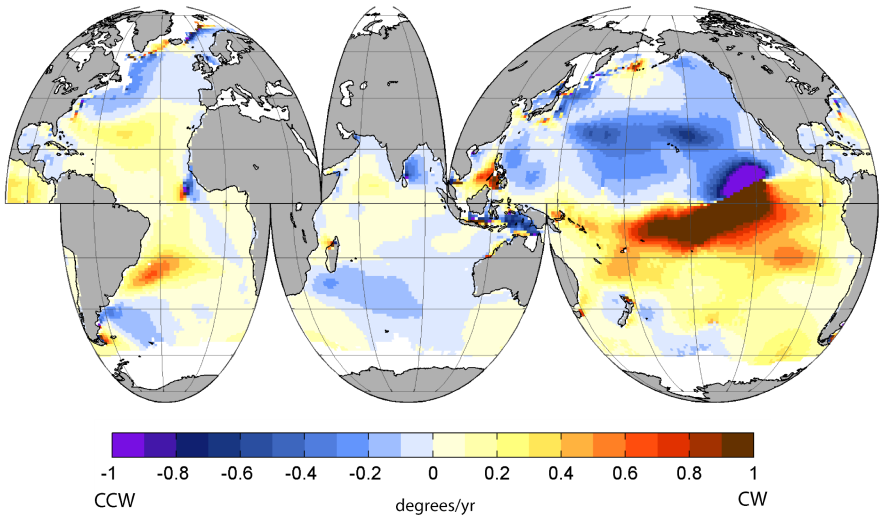

Figure 3.23: Annual long-term trends in energy flux mean direction (degrees/year), for the period from 1948 to 2008, computed through cylindrical regression. Data have been obtained from GOW wave database.

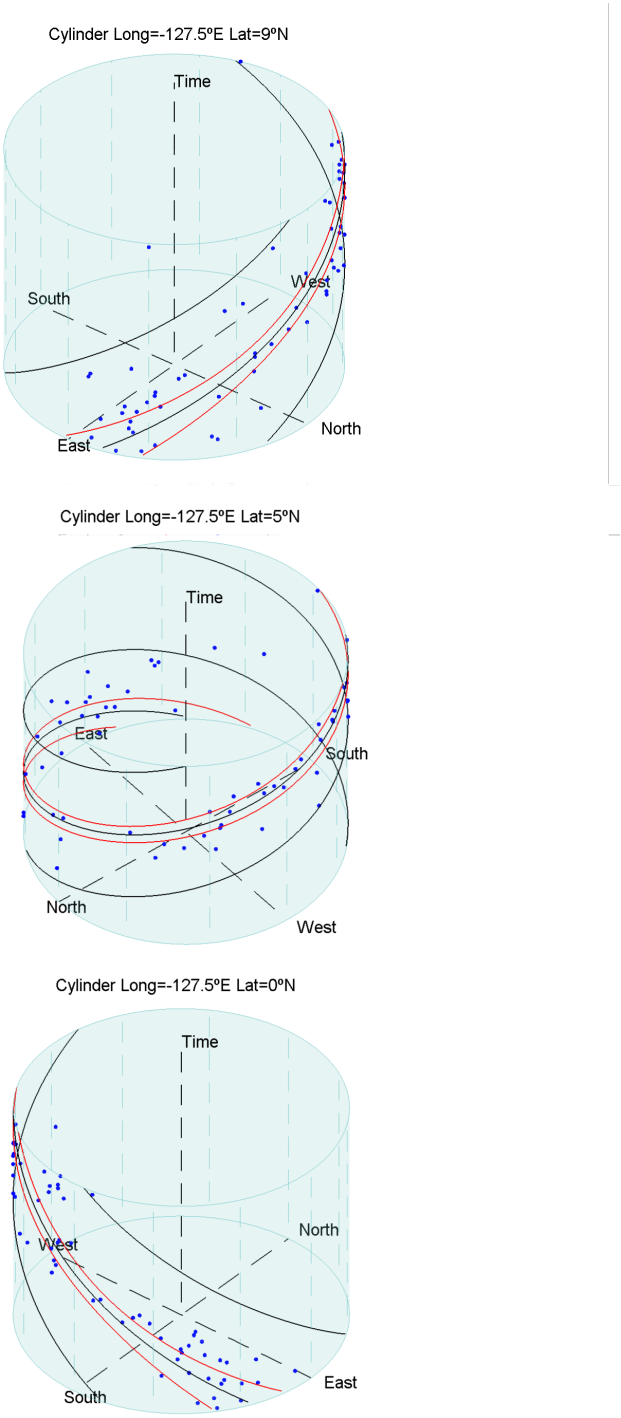

Figure 3.24: Trends (line) and data evolution in time (points) of the annual energy flux mean direction at a latitudinal transect in the mid Pacific, for the period from 1948 to 2008. Data have been obtained from GOW wave database.

In the North Pacific an extended counter-clockwise shift is found with values between -0.5 to -0.7 degrees/yr. In the North Atlantic significant changes around 0.3 are detected in the northern part becoming counter-clockwise shifts towards the equator, with a similar magnitude. The South-Atlantic basin is dominated by a clockwise shift between 0.2 to 0.3 degrees/yr. Regional features can be identified though.

The Indian basin shows weak shifts. However, the eastern South China sea and the Flores sea seem to have outstanding large shifts, around 0.7 degrees/yr, clockwise and counter-clokwise for each area, respectively.

A significant long-term trend has also been identified in the propagated (i.e. assuming Snell´s law) energy flux time series, depicted in Figure 3.25. Alongside this rotation in energy flux, coastal regions with sandy pocket beaches may have been affected in the long-term. Evidences of erosion/accretion rates have been reported but they are mostly related with climate patterns and inter-annual time scale.

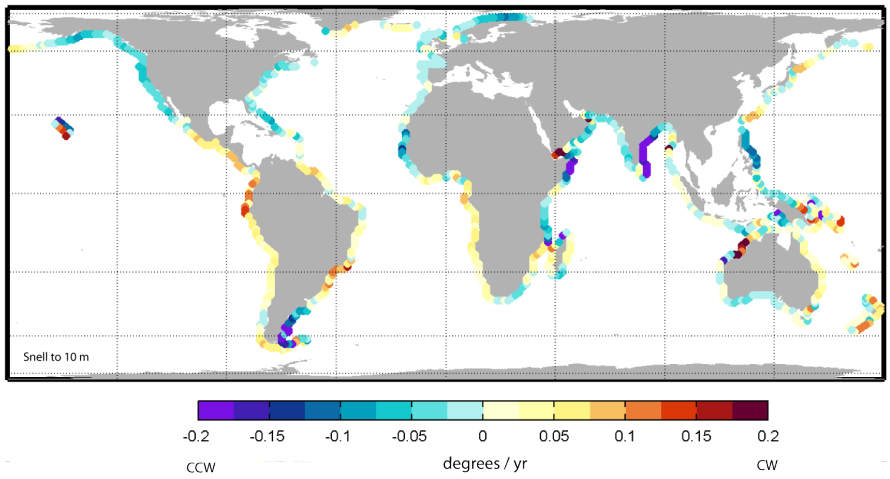

Figure 3.25: Long-term trend in the direction of mean energy flux at 10 m depth (propagated by Snell assuming straight and parallels contours depths; expressed in degrees/year).

Beach rotation occurs when sediment transport is restricted by the boundaries. Otherwise, the variation in sediment transport is the main factor altering the sediment budget. However, for longshore erosion, potential sediment transport depends mainly on variations in wave height and wave direction at the wave-breaking point. One of the most used expression to account for sediment transport in the surf zone is the CERC formula which relates the sediment transport with the wave incident direction as:

$$Q = \frac{0.39}{(\rho_s - \rho)g\lambda} \cdot \frac{1}{16} \cdot \rho g^{1.5} H_{sb}^2 .5\gamma^{-0.5} \sin 2\alpha_b \tag{3.6}$$

where ρ_s represents the sediment density, ρ the sea-water density, λ is the mean porosity, g the gravitational acceleration, α_b refers to the angle at the wave-breaking point with respect to the bathymetry and H_{sb} and γ are related through the breaking depth: $h_b = H_{sb}/\gamma$.

After propagating with Snell´s law and computing (on a hourly basis) the total CERC sediment transport rate (m^3/s) for each year from 1948 to 2008, the long-term trend in the total annual transport rate could be obtained, which is shown in Figure 3.26. Note that these results serve as indicators and a more detailed study is needed to provide further insight in the possible changes in the sediment transport derived from the changes in the wave climate at different time scales. Nevertheless, the results rise some concern on such an issue.

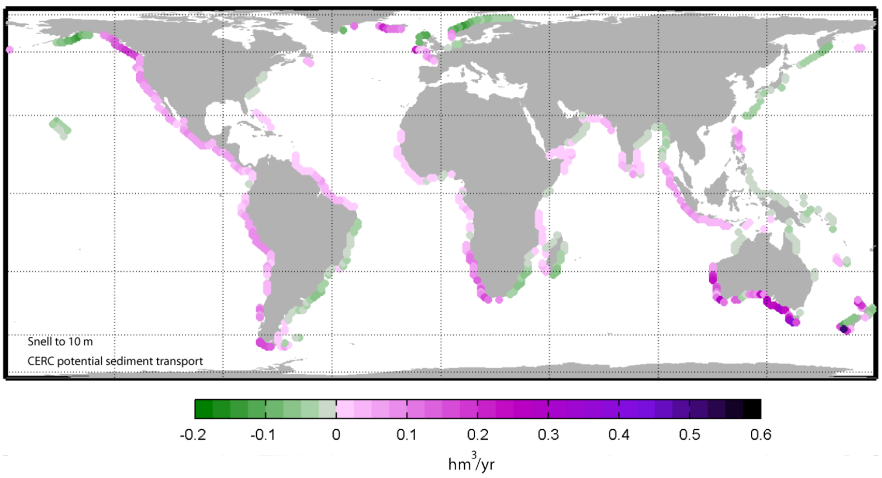

Figure 3.26: Long-term trend in potential sediment transport (CERC formula) at 10 m depth (propagated by Snell assuming straight and parallels contours depths; expressed in hm^3/year).

3.5.3 Long-term changes in the number of storms

Because observed changes in ocean wave heights can be used as an alternative metric of storminess ([Wang et al., 2009, Wang et al., 2011]), we use the Peak Over Threshold (POT) model ([Smith, 2001, Katz et al., 2002, Davison and Smith, 1990]) to identify the number of extreme wave events and their durations.

Two important issues that must be overcome when using POT approach is the selection of the threshold and the time span between two events to assure their independency. We adopt the 99.5^{th} percentile of the significant wave height as an adequate threshold given the length of the wave heights dataset ([Luceño et al., 2006]). The time span refers to the time interval to guarantee the independency between two consecutive storms. Following the recommendations in [Méndez et al., 2007] we choose 3 days as the minimum value for this interval. This is reasonable also for a global scale as Figure 3.27 shows that the mean duration of events in the global oceans are below this time span. Note that durations of events over 25 hours occur at the tropical areas of the oceans, related to trade winds in the Indian Ocean and swell propagation in the mid-Atlantic and mid-Pacific.

Because wave reanalyses show lower agreement in the intensity of the peak of the storms (higher dispersion of values with respect to measurements for high tail values, see [Reguero et al., 2012b]) here we use the number of exceedances over a threshold (i.e. number of storms) as an indicator of storminess because it can be considered to be well modeled in the dataset under analysis since the events sequence and occurrences are well represented in the input wind fields.

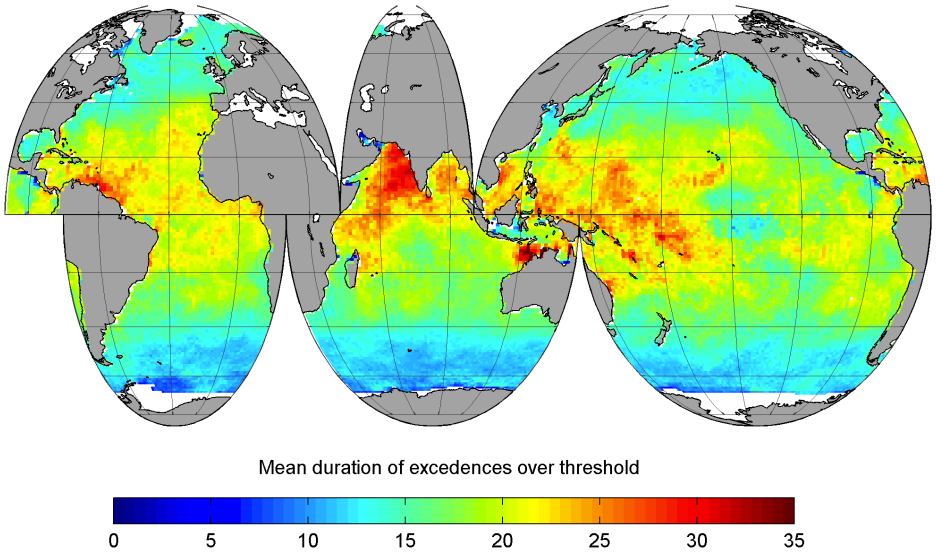

Figure 3.27: Mean duration of exceedances over threshold (in hours).

Once the number of events have been identified the number of exceedances per year are regressed against time and the statistic significance is verified with the t-test. Figure 3.28

displays the change in number of events with respect to the mean number of events per year. Maximum changes in number of events are found in the mid Pacific. A 5% of increase is detected in the eastern mid-Atlantic and south-western area. At mid latitudes, a decrease around 5% in the number of events is found at the same region where maximum negative trends have been detected (see Figure 3.20). This seems to indicate not only a reduction in wave heights but also in the number of extreme events. A moderate increase (around 2%) is also found in the northern Pacific, Southern Ocean, northern Indian basin and South-Atlantic, with a spatial concentration on the continental margins. Finally, a decrease of a 2% in the number of events is revealed to be occurring in the western tropical Atlantic.

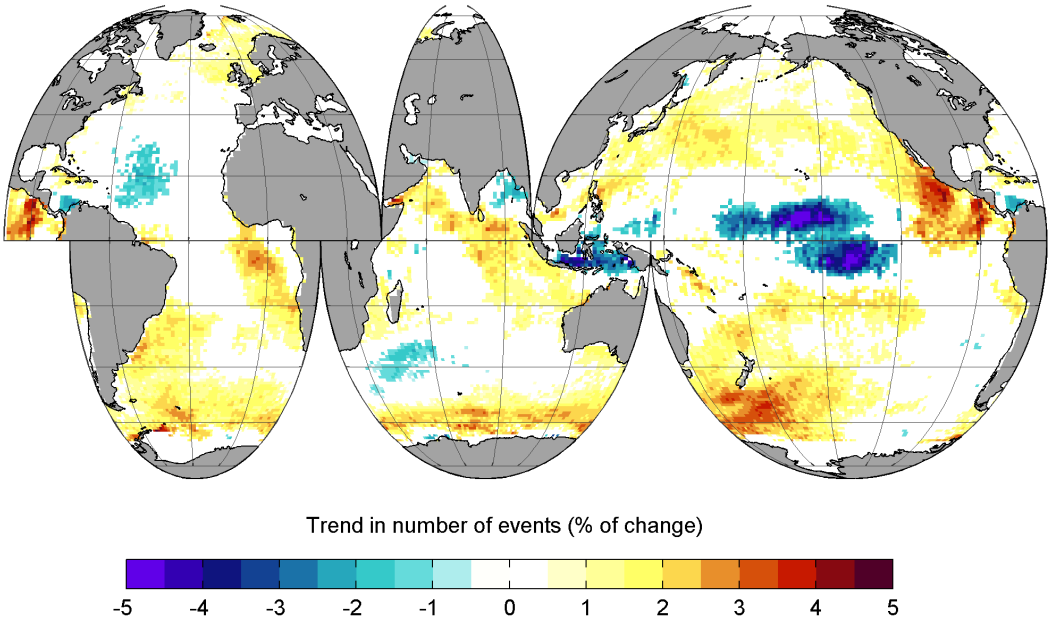

Figure 3.28: Trend in number of extreme wave events over a threshold with respect to annual mean number of storms (in percentage of change).

3.5.4 Long-term changes in wave extremes

To study the extreme wave heights and whether long-term changes are affecting them, a non-stationary wave extreme analysis is carried out at approximately 1,000 points along the world coastline. A generalized extreme value distribution (GEV) accounting for long-term factors in the distribution parameters was adjusted for the monthly maxima as explained in chapter 3. This is carried out with the statistical tool *IH-AMEVA*. Obtained results follow.

Figure 3.29 represents the wave height associated with a 100-year return period. It coincides with the results showed for the extreme wave heights in section 3.3.4 although in that case they corresponded to the annual maxima analysis which is computationally less demanding. When defining long-term changes a monthly maxima is preferred.

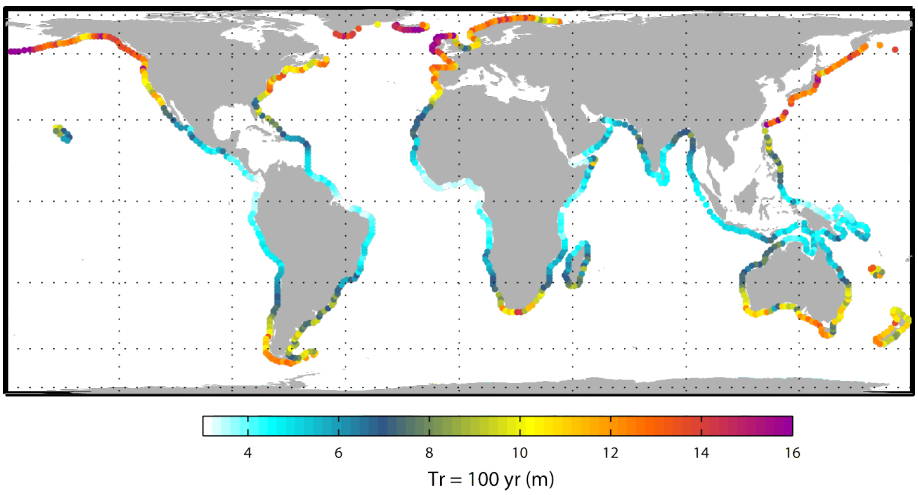

Figure 3.29: 100-yr significant wave height (H_s), computed for the period 1948-2008 from the GOW database.

In the analysis it was possible to determine the long-term trends, if significant, in the GEV distribution parameters. Figure 3.30 shows the results of the trend for the location parameter, which indicates how the distribution is being displaced. As seen, high latitudes are experiencing an increase from 1.5 to 2.5 cm/yr in the extreme wave heights as a rule. Tropical eastern coast of Asia, south-east margin of South America, and the western coast of North-America, from Mexico and northwards are some exceptions at low latitudes which are seeing an increase in wave heights as well.

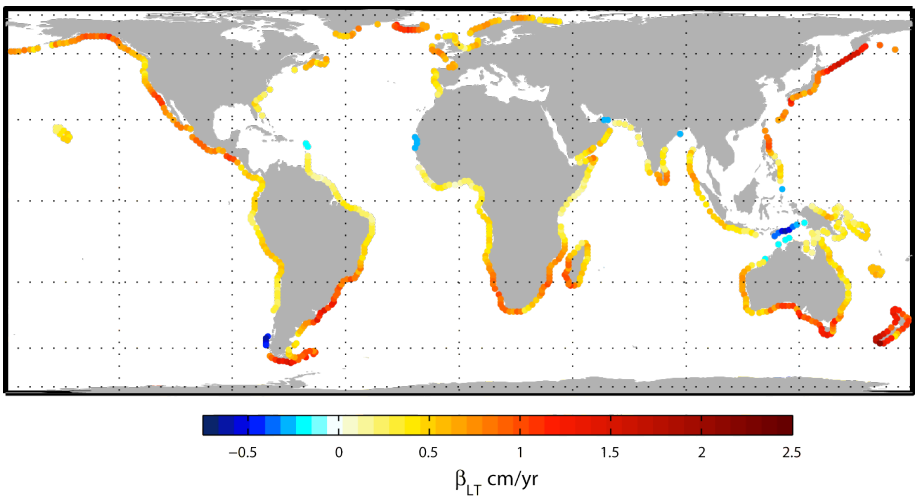

Figure 3.30: Long-term trend (cm/yr) in the significant wave height extremes, computed for the period 1948-2008 from the GOW database.

Should these changes occur, it is important to see what is the increase with respect to the dominant conditions rather than the magnitude of the increase. Figure **??** represents the

percentage of change due to long-term changes in the 61-years period with respect to the 100-yr H_s. The result is revealing. A larger relative increase is occurring the regions of California, south-east coast of South-America and eastern border of Asia. North Atlantic swells reaching tropical latitudes seem to be decreasing weakly. At the Flores Sea and certain parts of southern margin of Asia the decrease is larger. This visualization of the changes is more representative of possible coastal impacts due to changes in wave climate because these areas have been usually under milder extreme conditions. Proportionally, the rate of changes is of greater concern there.

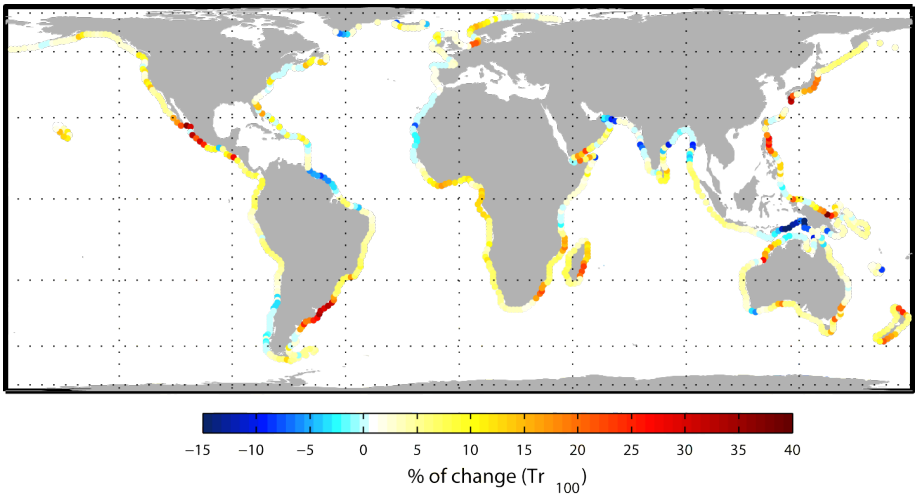

Figure 3.31: Percentage of change due to long-term changes in the 61-years period with respect to the 100-yr significant wave height. Computed for the period 1948-2008 from the GOW database.

3.6 Discussion on anthropogenically-forced changes in climate variability

3.6.1 Climate variability and long-term trends

Regarding the links and the contributions of the several climate indices to the wave climate seen previously, it would be interesting to see if changes in large climate patterns are being partially responsible of past trends. The fact is that previous trends and climate variability may be linked. [Hemer et al., 2010] partly attribute many of the trends found in the SH to a positive trend in SAM index over the past few decades ([Marshall, 2003]) and to an increase in the occurrence of El-Niño events.

Results in the last decades confirm a significant upward trend in wave heights in the North Atlantic and embedded within a pattern of multi-decadal variability over more than a century ([Gulev and Hasse, 1999, Gulev and Grigorieva, 2004]). Many of the changes in storms and waves over the last decades in the North-East Atlantic can be understood in terms of the behavior of the North Atlantic Oscillation (NAO). A recent strong trend in the NAO (towards stormier conditions) is apparently unique in its history, but it is controversial whether this is a response to greenhouse gas forcing ([Osborn, 2004]).

At present, confidence in Global Climate Models (GCM heareafter) and Regional Climate Models (RCM) modeled wind field changes is very low ([Hulme et al., 2002]). In light of the overall low confidence, a large number of analyses have been conducted and many GCM suggest a general trend towards the stormier tendency of the NAO in the 21st century (e.g. [Terray et al., 2004, Miller et al., 2006]). However, some Regional Climate Models suggest different and mostly weaker changes in winds and storminess (e.g. [Hulme et al., 2002, Barnett et al., 2006]). Overall climate models typically predict a decrease in the total number of extra-tropical cyclones, but an increase in the number of the most intense storms ([Lambert and Fyfe, 2006]). Either a strengthening of the storm track or an increase in intense cyclones will result in variations of wave conditions in the North-Atlantic ([Wolf and Woolf, 2006]).

3.6.2 Comments on ENSO phenomenon

ENSO is the most important global mode of climate variability with worldwide influence but with the strongest effect in the Pacific, and also one of the most prominent for wave climatology as seen previously. There are numerous summaries of the effects of global climate and climate variability on the tropical Pacific ([Rasmusson and Carpenter, 1982, Philander, 1982, Larkin and Harrison, 2001, Sarachik and Cane, 2010, Walsh et al., 2012]). The observed global climate warming over the past few decades has been hypothesized to have had some effect on ENSO, but firm attribution of anthropogenically-forced changes is lacking ([Collins et al., 2010]). Because unstable coupled systems that give rise to ENSO phenomenon can generate internal variability on decadal or centennial time scales that can resemble the effects of climate change, it is still unclear whether changes in the characteristics of ENSO over the past century have exceeded

its natural variability. Complicating the assessment is the presence of well-documented decadal variations in ENSO such as the Pacific Decadal Oscillation ([Mantua et al., 1997]) or its time filtered, Pacific-wide version of the Interdecadal Pacific Oscillation (IPO; [Power et al., 1999]). It is therefore difficult to say whether the observed global warming of the past century has altered ENSO and future simulations increase in complexity.

For future projections, GCM predictions of ENSO are also hampered, notwithstanding their considerable improvement during last decade ([Guilyardi et al., 2009]). Most models have a too strong equatorial wind stress zone that causes excessive upwelling along the equator and a persistent negative bias in simulated sea surface temperature (usually known as the "cold tongue bias"). Models also differ considerably in the future projections of ENSO ([Collins et al., 2010]) making it difficult to reach a consensus on its future behavior.

Regarding these facts, it becomes necessary to consider natural variability and long-term changes independently but not separately as they both configure a unique reality affecting wave climate and its induced impacts.

3.7 Global wave power

3.7.1 Global wave power and Climate Change, a connection?

Extratropical cyclones play a dominant role in the middle and high latitudes and any systematic change either in intensity, frequency or storm tracks position will have large influence in local climate conditions. In particular, over the global oceans, any change in these factors would affect global coast wave climate. The tendency for a poleward shift in extra-tropical cyclone activity by several degrees latitude in both hemispheres appears to be a consistent result of many studies emerging more recently ([Meehl et al., 2007]). The shift is associated with increased storm activity at higher and reduced storm activity at mid-latitudes. Possible explanations have been put forward for example by [Bengtsson et al., 2006] or [Yin, 2005] and are related to differential changes of the meridional temperature gradient with height and the resulting regional differences in changes in vertical stability. Generally, the poleward shift in extra-tropical storm activity appears to be more pronounced in the Southern Hemisphere ([Bengtsson et al., 2006]) which is consistent with the results found in our wave modeling study.

Several studies have analyzed storms tracks and climate change (e.g., [Carnell and Senior, 2002, Leckebusch and Ulbrich, 2004, Geng and Sugi, 2003, Bengtsson et al., 2006]). All these studies are based on the simulations of global circulation models and while some of them predict a reduction in the number of cyclones but an increase in their intensity; others indicate significant changes in storm tracks and, others, conclude that no significant change must be expected.

Alongside with this controversy, sea surface temperature (SST) gradients have been demonstrated to play a role in the position and activity of the storm tracks ([Inatsu et al., 2002, Inatsu and Hoskins, 2004]) in any case. [Inatsu et al., 2002] investigate the tropical and extratropical SST effects on mid-latitude storm tracks, finding that tropical SST forcing modulates

storm tracks distribution. Additionally, [Bengtsson et al., 2006] results show regional changes in storm tracks, being associated with regional SST changes: tropical areas affected by Rossby wave propagation, and the locking in of the storm tracks mechanism suggested by [Inatsu et al., 2002] in the extratropical SST.

In this section, we study the relationship between the global SST signal and the global wind-waves power over the last six decades. Linking a factor affecting storm tracks distribution with a direct quantity derived from them, such as the wave energy transferred to ocean waves, constitutes a newish approach to understand the possible changes under climate change scenarios.

3.7.1.1 Past trends in Wave power

From the late 1980s, the trend of increasing wave heights in the North Atlantic and other basins has been reported (e.g. [Carter and Draper, 1988, Bacon and Carter, 1991, Graham and Diaz, 2001, Menendez et al., 2008, Hemer et al., 2010, Dodet et al., 2010, Young et al., 2011]) North Atlantic and North Pacific have roughened over last decades. However, not a global signal has been determined yet. Chapter 4 will focus on the wave energy resource and its past changes. Along with other results, long-term trends will be explained.

Globally, wave power has been increasing during the last six decades. The annual wave power shows a clear increasing trend, displayed in Figure 3.32. This means that more energy is being transmitted to waves from wind in all the oceans on average. The implications for the design of wave farms is crucial because the WECs are designed for a certain range of wave power and results show that, in a global average, wave power has increased in about a 30% on the last 6 decades. This issue will be addressed specifically in the next chapter.

Figure 3.33 shows that the behavior is equivalent within seasons, showing a slight increase in the evolution for spring (MAM) and a milder slope in summer (JJA) which probably corresponds with different energy transfers in each hemisphere.

Despite these results, the exact rate of change in global wave power must be taken with caution as it is based on a numerical dataset that could be affected by inhomogeneities in the SH thus affecting the global average. Consequently, the correlation results will be compare below with altimeter data in the common time span.

3.7.1.2 Correlation of Wave Power with Sea Surface Temperature

Several papers have reported observed changes in extratropical cyclone activity over the second half of the twentieth century, which are characterized by a significant decrease in activity in the mid-latitudes and an increase in the high latitudes on the NH, suggesting a poleward shift of the storm track in winter (e.g., [McCabe et al., 2001, Gulev et al., 2001, Wang et al., 2006, Ulbrich et al., 2009]). The previous reported trends seem to have continued into the early twenty-first century ([Wang et al., 2011]).

The most important changes that are anticipated in the mid-latitude storm climate include: (1) a poleward shift of the mid-latitude storm tracks ([Meehl et al., 2007]), (2) an in-

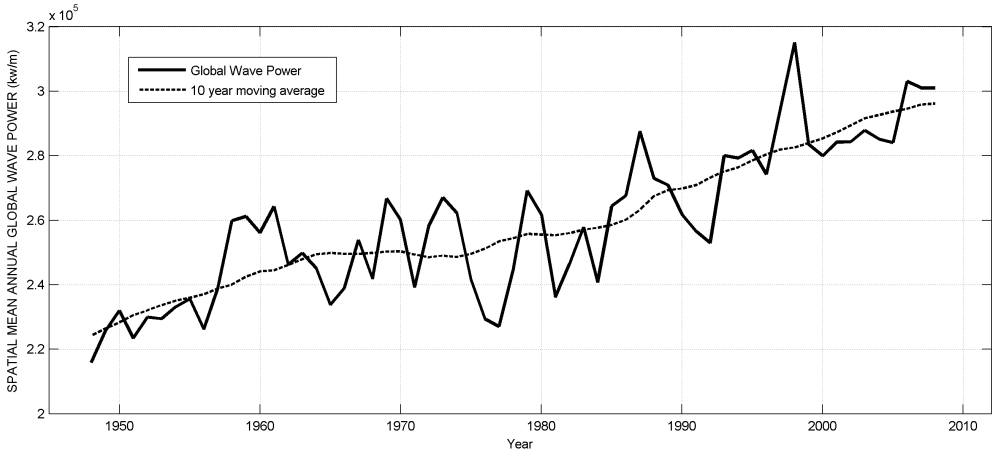

Figure 3.32: Globally averaged Wave Power signal and 10-yr moving average. Computed for the period 1948-2008 from the GOW database.

creased number of storms for certain regions (e.g., Great Britain, Aleutian Isles) and (3) a minor reduction in the total number of cyclones (e.g. [Ulbrich et al., 2009, Loeptien et al., 2008, Leckebusch et al., 2006, Lambert and Fyfe, 2006]).

Centennial time series of visual observations of surface wind waves have been analyzed to assess historical trends in ocean wave heights ([Gulev and Grigorieva, 2004, Gulev and Grigorieva, 2006]), which can be used as an alternative metric of storminess, corroborated by later studies ([Wang et al., 2006, Gulev and Grigorieva, 2006, Wang et al., 2008, Young et al., 2011, Semedo et al., 2011b]).

Global warming has increased the number and intensities of extratropical storms at high latitudes. Other climate characteristics affecting global ocean waves include variation in water temperature and atmospheric pressure anomalies that determinate the strength of the storms and inter-annual climate variations episodes.

Category 4-5 hurricanes show an increase since the mid-1940s ([Bender, 2010]) but these data need to be carefully assessed for homogeneities in the record ([Knutson et al., 2008]). Future projections based on theory and high-resolution dynamical models consistently indicate that greenhouse warming will cause the globally averaged intensity of tropical cyclones to shift towards stronger storms, with intensity increases of 2–11% by the end of the century. Existing modeling studies also project decreases in the globally averaged frequency of tropical cyclones by 6–34% ([Knutson et al., 2010]). Large amplitude fluctuations in the frequency and intensity of tropical cyclones greatly complicate both the detection of long-term trends and their attribution to rising levels of atmospheric greenhouse gases. The debate on whether past changes in tropical cyclone activity have exceeded the natural variability is still open ([Knutson et al., 2010]).

Increases in key measures of Atlantic hurricane activity over recent decades are believed to reflect, in large part, contemporaneous increases in tropical Atlantic warming (e.g., [Emanuel, 2005]). Some recent studies (e.g. [Goldenberg et al., 2001]) have attributed these

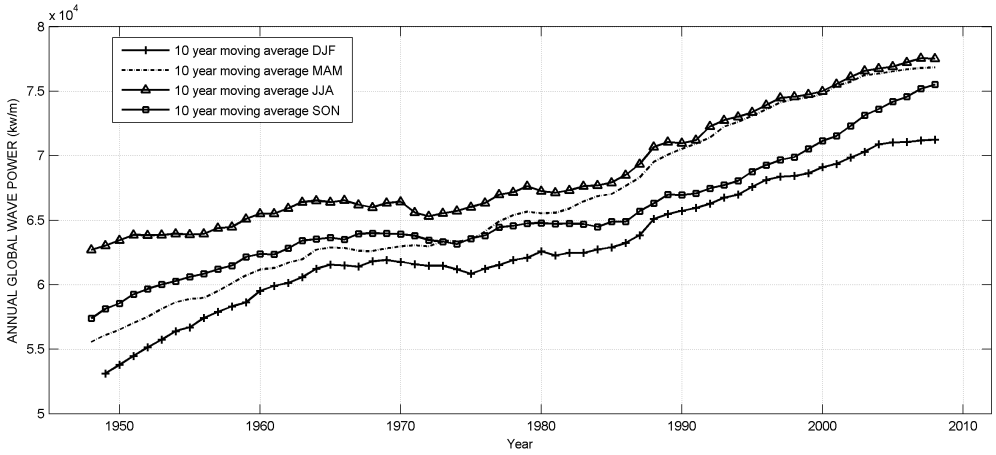

Figure 3.33: 10-yr moving average of seasonal globally averaged wave power. Computed for the period 1948-2008 from the GOW database.

increases to the Atlantic Multidecadal Oscillation (AMO), while other studies suggest that climate change may instead be playing the dominant role [Emanuel, 2005, Webster et al., 2005]). [Mann and Emanuel, 2006] presented results indicating that anthropogenic factors are likely responsible for long-term trends in tropical Atlantic warmth and tropical cyclone activity.

A measure of total power dissipation by tropical cyclones (the power dissipation index, or PDI) has been shown by [Emanuel, 2005] to be well correlated with the Sea Surface Temperature (SST) over the past half century, during which tropical cyclone wind measurements are most reliable. Other studies ([Vecchi et al., 2008]) noted that hurricane activity is also statistically correlated with other SST indices besides tropical Atlantic. However, the historical tropical storm count record does not provide compelling evidence for a climatic change induce long-term increase ([Landsea et al., 2006, Knutson et al., 2008]). In the case of global mean SST, the IPCC 4th Assessment Report (2007) present strong scientific evidences that most of the global warming observed is very likely caused by human greenhouse gas emissions over the past last half century.

Since teleconnections are important in forcing and transmitting climate signals globally, the focus here is to determine if climate change generates a remaining signal in ocean wave power as it does with other global variables like SST or Surface Air Temperature (SAT).

Global warming is well established through measurements of atmospheric and SST which have increased over the decades on average([**?**]). Of interest is if ocean water temperature has increased in parallel with the air temperature. This connection has a direct consequence to the potential increase in extra-tropical storms intensity. Being well established that during last decades SST has increased, whether there is a relationship with the global wave power (WP) signal is explored in the following.

SST data were obtained from the Extended Reconstructed Sea Surface Temperature (ERSST) NOAA database. It provides data on a monthly basis since 1950 and with a spatial resolution of 2^o in longitude and latitude for all the globe. These data were obtained from embedment of

buoy and satellite information in statistical modeling for spatial continuity. There are available data since 1880 but the signal shows higher confidence since the 50s. For more information in this regard the web: http://www.ncdc.noaa.gov/oa/climate/research/sst/ersstv3.php can be consulted.

SST global average signal has been correlated with the global average signal of wave power (WP) showing a linear correlation of 0.85. Both time series are represented in Figure 3.34. Latitudinal weighting was considered for the spatial average computation. The same analysis was performed for the SAT time series (Figure 3.36). In this case the linear correlation is of 0.76.

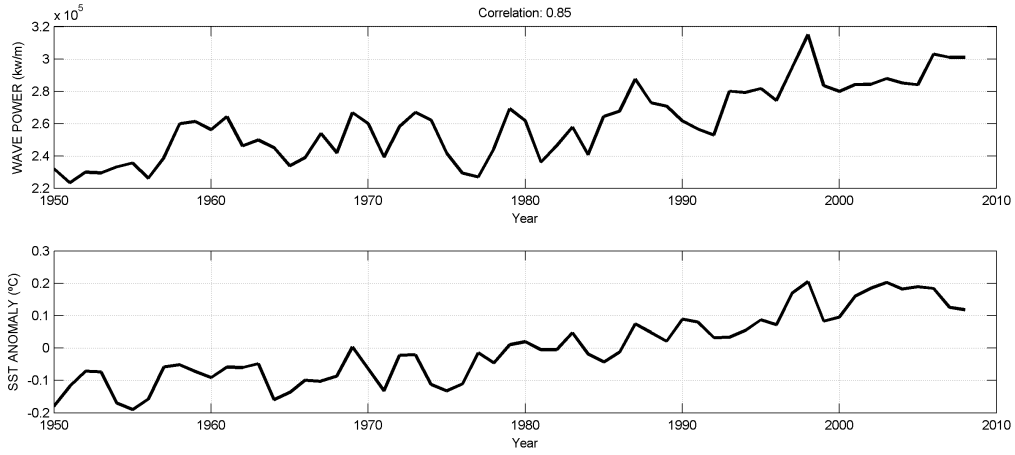

Figure 3.34: Time-series of global averaged Wave Power (WP) and Sea Surface Temperature (SST) showing the linear correlation between them.

Despite the high correlation the fact that the wave data come from a numerical source, and in awe of homogeneity problems in the SH within the different reanalyses, in Figure 3.35 the altimeter wave data have been included and the correlation with the numerical wave power computed. Some precautions were taken since the altimeter data are scatteredly distributed in space and time. To avoid the comparison with uniform distributed reanalysis data, the numerical results were interpolated in time and space to the altimeter data. The global signal were computed utterly for both samples of data (black and red dots in Figure 3.35). The resulting correlation is in this case of 0.77 in the altimeter time span. It is considerably high considering the short period of time analyzed. The time variability seems also to be adequately modeled in the GOW reanalysis.

Before reaching conclusions from these results, an additional step must be given. Linear correlation may be affected of auto-correlated noise that would mislead the analysis. Cross-correlation functions strongly depend on the structure of the original time series through auto-correlation, which implies that nonzero values of the cross-correlation function do no necessarily represent a relationship between two time series if they are auto-correlated ([Katz, 1988]).In order to avoid possible artificial cross correlations, a prewhitening of each time series is carried out. Prewhitening fits a p-order auto-regressive model (AR(p)) of the form:

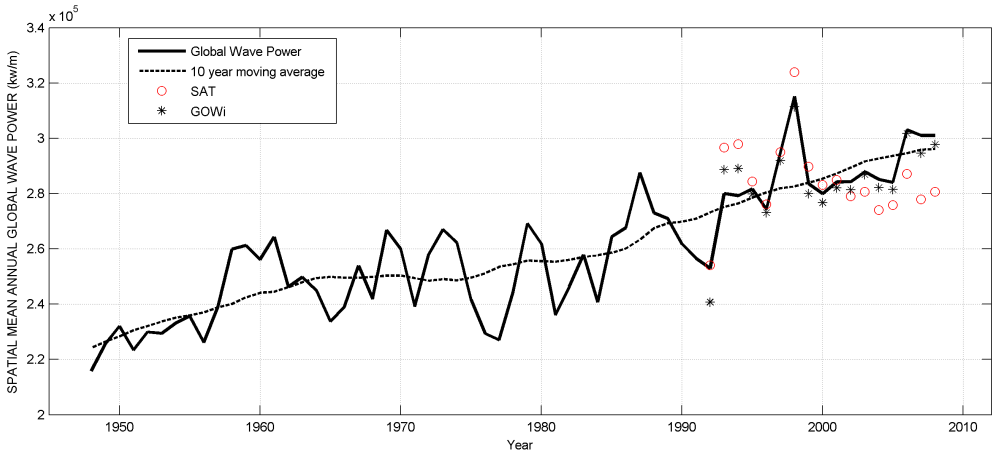

Figure 3.35: Globally averaged Wave Power signal and 10-yr moving average, including the altimeter data (red dots) and the corresponding GOWi data (black dots).

$$x(t) = a_1 x(t-1) + ... + apx(t-p) + \phi(t) \tag{3.7}$$

to the original time series, which is sufficient to reduce the residuals ($\phi(t)$) to white noise. The order of the auto-regressive is selected by Akaike Information Criterion ([Akaike, 1974]). The Akaike Information Criterion (AIC) determines the model order "p" by minimizing a theoretical information function given by,

$$AIC(p) = N \ln(\sigma_x^2(p)) + 2p \tag{3.8}$$

where N is the number of samples and $\sigma_x^2(p)$ is the estimated variance of the white driving noise and the term 2p in equation 3.8 is a "penalty" for the use of extra AR coefficients that do not substantially reduce the prediction error [Konyaev, 1990]. Once the value of the filter order "p" is obtained by minimizing the AIC criterion, the residuals obtained after fitting the AR(p) process in equation 3.7 are not auto-correlated time series.

The non auto-correlated series are represented in Figure 3.37. The correlation is in this case of 0.5 showing a clear relationship between both variables.

In the light of these results, it can be affirmed that SST global signal, reported to have being raised in the last decades, seems to be highly correlated with the increase in the wave power. The SAT does not show such a clear dependency. It was neither found in ocean basins nor in latitudinal bands (results not shown), which might be indicating that it is a global process enabled by climate teleconnections. Although a simple regression model could be easily built between the two variables, analogously to [Vermeer and Rahmstorf, 2009] for SLR, as a first approach to extending the consequences of SST future increase, the causes of such a relationship would need further analysis and are considered out of the scope of this work.

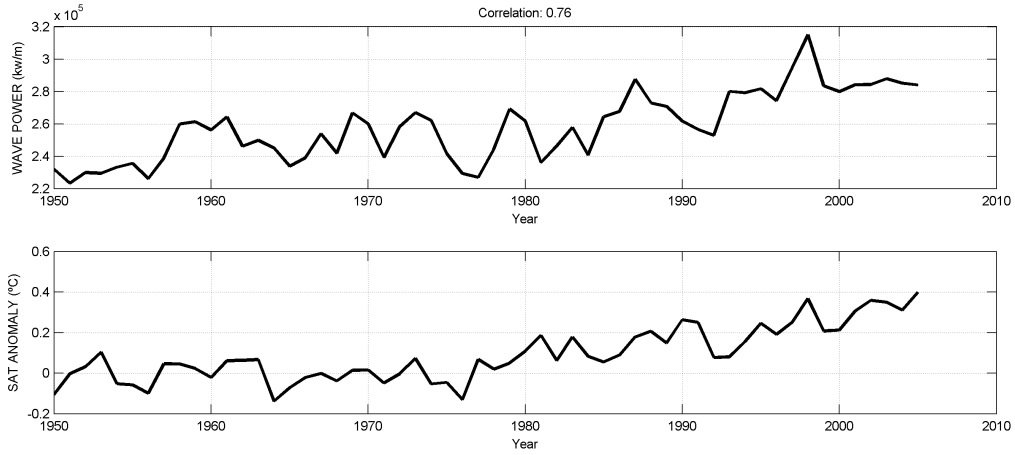

Figure 3.36: Time-series of global averaged Wave Power (WP) and Sea Air Temperature (SAT) showing the linear correlation between them.

3.8 Conclusions and discussion

The present analysis is aimed at determining long-term changes in the global wave climate (in the period from 1948 to 2008) combined with the study of inter-annual correlations. Prior to it, a description of global climatology, similar to other works, is provided. Special focus is given to the description of periods, important for wave energy assessment, and to the directional behavior of wave climate. These last two features have been less attended in current state of art.

In this respect, it is confirmed that during the Austral winter the swell waves coming from the Southern Ocean dominate these areas provoking large shifts in the time series of energy flux direction. This occurs due to the widening and strengthening of the storms in the SH and the weakening in the NH. This behavior has also been reflected in the seasonal variations analyzed in this work.

Concerning the variability of wave climate, wave heights, mean energy flux direction and wave power have been studied in relation with many of the most influencing climate patterns in the globe. From this analysis, consequences for coastal areas and an quantification of the mean contribution to wave climate parameters have been inferred. Rates of change and variation of wave climate in time are necessary to be considered in coastal hazardous areas.

In general terms, results have shown that not only the mean values are increasing but also the high tail of the H_s distribution values does. Moreover, trends for the 90^{th} percentile are more intense than for the mean values, while coinciding with lower correlation with climate indices. However, there are regions of the oceans where extreme values are increasing and mean conditions are not. Such are the cases of the southern Atlantic or the northwestern Pacific. Differences are also identified in the North Atlantic where no significant changes are obtained but at the northern area.

Surprisingly, the trend pattern obtained for the available satellite period significantly differs

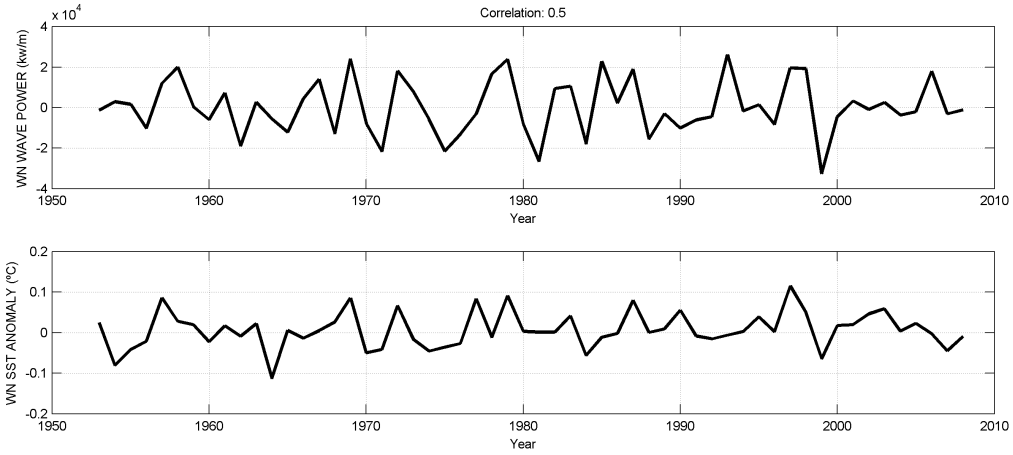

Figure 3.37: Correlation after prewhitening between wave power and Sea Surface Temperature global averaged time series. Latitudinal correction included.

from that computed for the last six decades. This fact indicates that longer time span in observations is needed to obtain meaningful trends of change in wave height parameters from satellite altimetry. As a consequence, no trend patterns should be obtained from this data source so far.

The analysis here developed also reveals that not only wave heights are increasing but also the number of extreme events at several areas of the global ocean. Additionally, the proportional change in the extreme intensities is not uniform throughout the global ocean.

The question of possible changes in the directional behavior of the dominant wave energy has been here explored. Sustained changes in the storm activity in both hemispheres are inducing large shifts of the mean energy flux direction clockwisely in the south and counter-clockwisely in the north. Greater shifts seem to be occurring in the mid Pacific with changes of more than 1 degree/yr. The directional trends were obtained from a regression model for directional data specifically designed for this purpose in this work owing to the lack of such modeling in this field.

Inter-annual variability is studied by obtaining the correlation patterns with the most prominent climate indices. The Artic Oscillation and the Southern Annular Mode are the most influencing climate patterns in the Northern and Southern Hemisphere, respectively. The correlation was obtained for the mean wave heights and a high percentile. Results show that the influence is greater for mean conditions. The contribution of the presence of each climate pattern (i.e. per unit of standardized index) has been shown that could be in the range of a 10% in large areas of the oceans and even exceeding a 25% in some regions in particular. The influence varies spatially and in magnitude within the year but the relative contribution is sustained in a great proportion.

The inter-annual correlation patterns were also obtained for the anomaly of the mean energy flux direction obtaining clear evidences of shifts with some climate patterns. Southern Annular Mode controls the direction of wave energy in the Southern Hemisphere as already shown by

previous research. However, the North Atlantic Oscillation, the Artic Oscillation and the Pacific North American Index seems to hold great influence in the Northern Hemisphere. This information is a good basis for further modeling on inter-annual influence of beach rotation, coastal flooding and sediment transport variations in the global coast.

Finally, the analysis carried out has led to a surprising finding. It seems to exist a global increase in the ocean wave power in the last decades. In principle, such sustained change could be attributed to the numerical origin of the data or possible inhomogeneities. The former can not be discarded but this increase is strongly correlated with the Sea Surface Temperature though. Results have been confirmed with satellite wave data in the available altimeter period. The causes of this relationship and whether it allows future extrapolation of wave power from variations in sea surface temperature needs further insight. Ocean and storm activity are indeed linked and, provided this relationship is confirmed, wave energy could become an indirect measure of the climate change effect on storm activity.